ROLE OF BAUSCHINGER EFFECT IN THE TRANSIENT OBSERVED IN TENSION AFTER TORSIONAL PRESTRAIN IN SOME METALS

by

V. THIRUVENKATA SWAMY

DEPARTMENT OF METALLURGICAL ENGINEERING

INDIAN INSTITUTE OF TECHNOLOGY, KANPUR

JULY, 1982

ROLE OF BAUSCHINGER EFFECT IN THE TRANSIENT OBSERVED IN TENSION AFTER TORSIONAL PRESTRAIN IN SOME METALS

A Thesis Submitted
In Partial Fulfilment of the Requirements
for the Degree of
MASTER OF TECHNOLOGY

by

V. THIRUVENKATA SWAMY

to the
DEPARTMENT OF METALLURGICAL ENGINEERING
INDIAN INSTITUTE OF TECHNOLOGY, KANPUR
JULY, 1982

ME-1982-M-SWA-ROL

CERTIFICATE

Certified that the present work "Role of Bauschinger Effect in the Transient Observed in Tension After Torsional Prestrain in Some Metals" has been carried out by Mr. V. Thiruvenkataswamy under my supervision and has not been submitted elsewhere for a degree.

G.S. Murty
Professor & Head
Department of Metallurgical Engineering
Indian Institute of Technology
KANPUR.

July, 1982

ACKNOWLEDGEMENTS

I wish to express my gratitude and sincere thanks to Dr. G.S. Murty for his guidance throughout the course of this work.

I would like to acknowledge the immense help rendered by Mr. B.K. Jain, Materials Testing Lab, A.C.M.S.

I would also like to thank my friends S/s J.K. Murty, Y.R. Shanker, G.V. Srinivasan and S. Chandrashakeran for their timely help and encouragement during this work.

My thanks are also due to Mr. R.N. Srivastava and Mr. R.S. Dubey in the preparation of this manuscript.

TABLE OF CONTENTS

		Page
LIST OF TABLES		vi
LIST OF FIGURES		vii
ABSTRACT		ix
1.	INTRODUCTION	1
1.1	Review of twist prestrain effect on single crystals	1
1.2	Review of twist prestrain effect on poly-crystals	2
1.3	Bauschinger effect and its measurement	5
1.4	Bauschinger effect in single and poly-crystalline materials	8
1.5	Theoretical models to explain Bauschinger effect	10
1.6	Scope of the present investigation	13
2.	EXPERIMENTAL PROCEDURE	16
2.1	Specimen preparation	16
2.2	Mechanical testing	17
3.	RESULTS	22
3.1	Torsion-tension test	22
3.2	Tension-compression tests	23
3.3	Comparitive study of torsion-tension and tension-compression tests	24
3.4	Torsion-reverse-torsion tests	25
3.5	Tension-torsion-tension tests	26
3.6	Specimen diameter effect in torsion-tension tests	27

Page

3.7 Tensile tests on carburised mild steel samples 27

4. DISCUSSION 29

5. CONCLUSIONS 33

REFERENCES

LIST OF TABLES

		Page
I	Torsion-Tension Test	35
II	Torsion-Tension Tests on 6 mm Diameter Mild Steel Samples	36
IIIa	Torsion-Tension Test on 4 mm Diameter Copper Samples	37
IIIb	Torsion-Tension Test on 6.5 mm Diameter Copper Samples	38
IV	Torsion-Tension Test on 6.4 mm Diameter Aluminium Samples	39
V	Torsion-Tension Tests on Mild Steel Samples	40
VI	Torsion-Tension Tests on Copper Samples	40
VII	Torsion-Tension Tests on 6.4 mm Diameter Aluminium Sample	41
VIII	Tension-Compression Tests on Annealed Mild Steel Sample	41
IX	Tension-Compression Tests on Mild Steel	42
X	Tension-Compression Tests on 6 mm Diameter Copper Samples	42
XI	Tension-Compression Tests on Copper Sample	43
XII	Torsion-Reverse-Torsion Tests on 6 mm Diameter Mild Steel Samples	44
XIII	Torsion-Reverse-Torsion Test on 6.5 mm Diameter Copper Sample	45
XIV	Tension-Torsion-Tension Tests on 6 mm Diameter Mild Steel Samples	46
XV	Tensile Test of Carburised 6 mm Diameter Mild Steel Samples	47

LIST OF FIGURES

1	Bauschinger Effect Factors
2	Specimen Dimension Specification for Various Type of Tests
3(a) & (b)	True Stress-Strain Curves of Twisted, 6 mm Diameter Mild Steel Specimens in Tension
4	True Stress-Strain Curves of Twisted, 4 mm Diameter Copper Specimens in Tension
5	True Stress-Strain Curves of Twisted, 6.5 mm Diameter Aluminium Specimens in Tension
6	Prestrain versus Bauschinger Stress in Mild Steel Specimens
7	Prestrain versus Bauschinger Strain in Mild Steel Specimens
8	Prestrain versus Bauschinger Energy in Mild Steel Specimens
9	Prestrain versus Bauschinger Stress in Copper Specimens
10	Prestrain versus Bauschinger Stress and Bauschinger Strain in Torsion-Tension Test of Copper
11	Bauschinger Stress versus Rate of Work-hardening in Mild Steel
12	Bauschinger Strain and Bauschinger Energy versus Rate of Work-hardening in Mild Steel
13	Bauschinger Stress versus Rate of Work-hardening in Copper
14	Bauschinger Strain and Bauschinger Energy versus Rate of Work-hardening in Copper
15	Tension-Compression Test on Mild Steel
16	Tension-Compression Test on Copper
17	Torsion-Reverse Torsion Test on Mild Steel

18	Torsion-Reverse Torsion Test on Copper
19	Tensile Tests of Combined Prestrained Mild Steel Specimens
20	True Stress-Strain Curves of Twisted, 4 mm and 6.5 mm Diameter Copper Specimens in Tension
21.	True Stress-Strain Curves of Twisted, 4 mm and 6,5 mm Diameter Copper Specimens in Tension
22	True Stress-Strain Curves of Carburised Mild Steel Specimens in Tension
23	Work-hardening Rate at Various Offset Strain Values in Carburised Mild Steel and Twisted Mild Steel Specimens
24	Tensile Tests With and Without Extensometer on Twisted, 6.4 mm Diameter Aluminium Specimens
25	Hardness Number versus Radial Distance in 6 mm Diameter Twisted Mild Steel Specimen
26	Hardness Number versus Radial Distance in 6 mm Diameter Carburised Mild Steel Specimen

ABSTRACT

Several studies have been made on single and poly-crystals to understand the tensile flow behaviour of twisted samples. It was observed that the initial flow stress, strain-hardening rate,ductility, reduction in area and nature of the failure are affected by the torsional prestrain. The high work-hardening rate and initial raise in flow stress due to torsional prestrain have been explained in terms of 'Strain inhomogeneity' and 'Bauschinger effect'. Additional experiments have been performed in this investigation in order to assess the above two interpretations for the torsional prestrain effect.

In this study, tests were performed on mild steel (0.13% C), commercially pure copper and commercially pure aluminium. The correlation between the Bauschinger effect and the high strain-hardening rate due to torsional prestrain has been widely explored. It was observed that the magnitude of Bauschinger effect shown by tension-compression test is greater than that shown by torsion-tension test for the same prestrain value. For the same Bauschinger effect the torsion-tension test shows higher work-hardening rate than the tension-compression test. Thus, the results show that the correlation between Bauschinger effect and work-hardening rate is not in conformity with the interpretation that torsional prestrain effect in tension is a consequence of Bauschinger effect.

Tensile tests were also performed on mild steel specimens carburised to different depths. In these tests, on specimens with a soft core and a hard case, a region of high work-hardening rate has been observed initially analogus to tensile tests on twisted specimens.

CHAPTER 1

INTRODUCTION

The usefulness of metals as structural materials depends primarily on the combination of their high strength and ductility. It is well known that plastic properties of metals are structure sensitive and thus the type and extent of plastic prestrain significantly influence the plastic properties. Some of the common methods of introducing plastic strain in metals are tension, compression and torsion. So far extensive studies have been carried out in order to understand the cold worked state of metals and yet much remains to be done in this regard.

The present investigation is concerned with changes in mechanical properties of metals in terms of Bauschinger effect as a result of abrupt changes in the mode of mechanical testing from torsion to tension, tension to compression and forward to reverse twisting in torsion at various prestrain levels. In this chapter the twist prestrain effect on tensile behaviour and Bauschinger effect are reviewed briefly from the literature and this followed by scope of present investigation.

1.1 REVIEW OF TWIST PRESTRAIN EFFECT ON SINGLE CRYSTALS

Paxton and Cottrell (1), Rebstock (2), Holt (3), Basinski and Basinski (4), and Osborne (5) conducted experiments on single crystals and observed that twist prestrain led to a raise in the flow stress.

Paxton and Cottrell (1) and Rebstock (2) reported that a twist during stage I of the stress-strain curve increased the hardening rate. In the stage II Rebstock (2) found that twisting led to transient reduction in the hardening rate. On the other hand, Paterson (6) observed a hardening rate lower than stage I in crystals that had been twisted before straining in alternative tension and compression.

In order to generalise the results comparisons of hardening rates before and after twisting for a particular flow stress were made. In general, the effect of twisting a single crystal is to increase the flow stress and decrease the rate of hardening in subsequent tensile test.

1.2 REVIEW OF TWIST PRESTRAIN EFFECT ON POLYCRYSTALS

Swift (7), Korber (8), Hollowman (9), Mehringer (10), Lynch (11), Fanpel (12) and Bridgeman (13) performed experiments on polycrystalline samples and observed that the effect of twist prestrain is to raise the initial flow stress and to increase the initial rate of strain hardening.

Swift (7) conducted experiments on mild steel samples and observed that the tensile behaviour upto 5 percent strain is affected by the twist prestrain. It was also found that if the torsional prestrain exceeded a certain value, the specimen failed in a brittle manner when subsequently loaded in tension, the fracture being distinctly different from the normal cup and cone failure observed at smaller twist prestrain.

Vaidya and Murty (14) have studied the twist prestrain effects on the tensile behaviour of polycrystalline copper of 99.99% purity. They observed that the rise in the flow stress is followed by a region of increased rate of strain-hardening as compared to the rate in an annealed sample at an equal flow stress. The extent of high initial hardening rate is found to depend on the twist prestrain. They suggested that this twist prestrain effect is due to strain inhomogenity across the cross section of twisted cylindrical bar. When a cylindrical bar is subjected to twist, the shear strain varies from centre to the periphery, the strain is minimum at the centre and maximum at the periphery. So due to this kind of strain gradient the dislocation density and hence the flow stress are expected to be maximum at the case region than that of core. When such a material (twisted one) is subsequently tested in tension, in order to maintain same amount of tensile plastic strain throughout the cross section the rapid dislocation multiplication will take place at the soft core region which results in very high initial work hardening. Once the dislocation density gradient gets eliminated then the work-hardening rate at this stage is expected to be same as that of material that has been prestrained to the same flow stress by tensile test alone.

On the other hand, Watson and Brown (15) have made similar kind of observations on commercial reinforced grade steel and interpreted their observations in terms of Bauschinger effect. According to them, at high twist prestrain both the

elastic core and more lightly work hardened region occupy a decreasing proportion of the total cross sectional area of the specimen and hence strain inhomogenity does not seem to contribute markedly to the macroscopic work-hardening rate, especially at highest twist prestrains. They suggested that twist prestrain effect in the tensile behaviour is a manifestation of Bauschinger effect and its elimination or reduction by straining leads to a rapid increase in flow stress and a very high apparent work-hardening rate. The observed high work-hardening rate thus results from the rapid immobilisation of dislocation which, because of the Bauschinger effect, require relatively low stresses to move. They observed that Bauschinger stress increase with work-hardening rate in torsion-tension tests. According to them the observed phenomenon is more general and not restricted to torsional prestrain.

Rao and Murty (16) performed a comparitive study of the torsional prestrain effect on the subsequent tensile behaviour and tensile prestrain effect on the subsequent compressive behaviour on mild steel, copper and aluminium with a view to assess the role of Bauschinger effect in explaining the observed region of high strain hardening rate in tension following torsional prestrain. They observed that the Bauschinger effect in torsion-tension tests is lower than that of tension-compression tests and the strain hardening rate in the transition region is higher in the former case. They concluded the lack of correlation between the magnitude of Bauschinger effect and the strain hardening rate in the transition region

is incompatible with the interpretation that the region of high strain hardening rate in tension following torsional pre-strain is a consequence of Bauschinger effect.

1.3 BAUSCHINGER EFFECT AND ITS MEASUREMENT

The directional dependence of yield and flow behaviour of cold worked state of metals is known as Bauschinger effect (17). Bauschinger effect has been defined in numerous ways by different investigatiors. In general,the most common way of defining the Bauschinger effect is, "The lowering of the yield stress due to an abrupt change in the direction of deformation". Since it is used as a design parameter in the structural and material fabrication processes, some kind of quantitative parameter is necessary to measure Bauschinger effect. Various quantities involved in the measurement of Bauschinger effect are illustrated in Figure 1 and the details of those factors are as follows.

(i) Bauschinger Stress '$\Delta\sigma$' is the numerical difference in the yield point (the point of unloading is taken as forward yield σ_F and offset yield or deviation from linearity in the reverse direction taken as reverse yield σ_R) between forward (σ_F) and reverse (σ_R) directions as measured in simple tension-compression tests, i.e.

$$\Delta\sigma = \sigma_F - \sigma_R$$

(ii) Bauschinger Strain 'β' is the plastic strain required to bring the yield point in reverse direction equal to forward yield or fixed fraction of forward yield stress in tension-compression tests. Here the point of unloading in the forward direction is taken as forward yield.

(iii) Bauschinger Energy 'E_s' is the energy saved in achieving a certain amount of deformation in reverse loading, as compared with the energy which would have been required to achieve the same increment of deformation in the absence of a Bauschinger effect. The above three factors are fundamental factors used to measure Bauschinger effect. The studies to measure Bauschinger effect on Zn crystals and Al-Cu alloys shows that Zn crystal has larger Bauschinger strain than Al-Cu alloys and at the same time Al-Cu alloys shows larger Bauschinger stress than that of Zn crystals. So Abel and Muir (16) introduced three Bauschinger parameters (β_σ, β_ε and β_E) to find better ways of describing and evaluating all aspects of the Bauschinger effect which are as follows

(iv) Bauschinger Stress Parameter 'β_σ' is the ratio of the Bauschinger stress to the forward yield stress in tension-compression test. The point of unloading in forward direction is taken as forward yield σ_F.

$$\therefore \quad \beta_\sigma = \frac{\Delta\sigma}{\sigma_F}$$

(v) Bauschinger Strain Parameter 'β_ε' is the ratio of Bauschinger strain to the plastic pre-strain value ε_F

$$\therefore \quad \beta_\varepsilon = \frac{\beta}{\varepsilon_F}$$

(vi) Bauschinger Energy Parameter 'β_E' is the ratio of Bauschinger energy and the energy (E_p) expanded in prestrain

$$\beta_E = E_s/E_p$$

Based on their observations, Abel and Muir (18) concluded that the Bauschinger energy parameter is the most important parameter to describe the effect, since it relates both stress and strain.

Some of the other ways in which Bauschinger effect is characterized are as follows.

(vii) Ibrahim and Embury (19) defined a Bauschinger effect parameter (B.E.P.) as

$$\frac{\sigma_F - \sigma_R^*}{\sigma_F - \sigma_o}$$

where σ_F and σ_o are forward and initial yield respectively and are generally measured by offset strain method. σ_R^* the reverse yield was not determined by the offset strain method but by back extrapolation to the elastic line from some linear part on the plastic portion of the reverse flow curve.

(viii) Bauschinger Effect Factor 'BEF' is the ratio of yield point in the reverse and forward direction

$$BEF = \frac{\sigma_R}{\sigma_F}$$

(ix) The Mean Internal Stress 'τ_i') from Bauschinger effect has been suggested by Orowan (20) and supported by Wilson's(21) work determining the internal stress with X-rays during the Bauschinger test

$$\tau_i = \frac{\sigma_F - \sigma_R^*}{2}$$

where σ_F is the flow stress in the forward direction and σ_R^* is the stress obtained by extrapolating the linear part of plastic curve in reverse direction to zero reverse strain.

Based on these Bauschinger factors, certain aspects of Bauschinger effect are reviewed from literature in the following section.

1.4 BAUSCHINGER EFFECT IN SINGLE AND POLYCRYSTALLINE MATERIALS

Several studies of Bauschinger effect have been reported in single as well as in polycrystals. The work (22) on Al single crystal shows that Bauschinger strain depends upon crystal orientation. The observations made by Buckley and Entwistle (23) in single and polycrystal specimens of high purity aluminium show that in single crystals, the Bauschinger strain is large at small strains and at high strains this effect in polycrystals is double that of single crystals. In poly-

(viii) Bauschinger Effect Factor 'BEF' is the ratio of yield point in the reverse and forward direction

$$BEF = \frac{\sigma_R}{\sigma_F}$$

(ix) The Mean Internal Stress 'τ_i') from Bauschinger effect has been suggested by Orowan (20) and supported by Wilson's(21) work determining the internal stress with X-rays during the Bauschinger test

$$\tau_i = \frac{\sigma_F - \sigma_R^*}{2}$$

where σ_F is the flow stress in the forward direction and σ_R^* is the stress obtained by extrapolating the linear part of plastic curve in reverse direction to zero reverse strain.

Based on these Bauschinger factors, certain aspects of auschinger effect are reviewed from literature in the following ection.

4 BAUSCHINGER EFFECT IN SINGLE AND POLYCRYSTALLINE MATERIALS

Several studies of Bauschinger effect have been reported ngle as well as in polycrystals. The work (22) on Al crystal shows that Bauschinger strain depends upon l orientation. The observations made by Buckley and le (23) in single and polycrystal specimens of high aluminium show that in single crystals, the Bauschinger s large at small strains and at high strains this effect ystals is double that of single crystals. In poly-

crystalline materials, the work on Cu, Al, Pb, Ni and Fe by Wolley (24) shows that Bauschinger effect is largely independent of grain size and Bauschinger strain is inversly proportional to the elastic modulus of the material. Numerous studies have been performed to understand the prestrain dependency of Bauschinger effect in polycrystalline materials. The work on mild steel by Abel and Muir (18) shows that Bauschinger stress, Bauschinger strain, Bauschinger energy and Bauschinger stress parameter increase with increasing prestrain, whereas Bauschinger strain parameter and Bauschinger energy parameter decrease with increasing prestrain. On the basis of the observations on Cu, α-brass, Fe, steels, Ti, Zn and Mg, Kishi and Gokyu (25) gave a mathematical relation between Bauschinger stress and plastic prestrain as

$$\Delta\sigma = K \varepsilon_p^m$$

where $\Delta\sigma$, ε_p, K and m are Bauschinger stress, prestrain, Bauschinger coefficient and Bauschinger effect exponent respectively. Here K and m are material constants. On the other hand, Gupta and Kodali (26) derived another kind of expression based on their observations on pure vanadium, annealed medium carbon steel, aged cupronickel alloy containing Si and Al-4 wt. % Cu alloy aged to produce θ' phase as

$$\Delta\sigma = m \ln \varepsilon_p + K$$

where $\Delta\sigma$ and ε_p are Bauschinger stress and plastic prestrain respectively, m and K are material constants.

Precipitation hardened single and polycrystalline aluminium alloys were studied by Abel et.al (27) and Stoltz et.al (28) respectively. In alloys with deformable precipitates, i.e., G.P. zones or θ'', the Bauschinger effect was small in magnitude comparable to that in pure aluminium. A much larger Bauschinger effect was observed in alloys with strong non-deformable second phases, such as θ' and θ. The Bauschinger effect in Al single crystals dispersion-hardened with silicon particles was studied by Matsuura et.al (29). It was observed that the mean internal stress estimated from the Bauschinger effect increased initially with prestrain until a critical strain ε_c and then appeared to saturate with increasing prestrain. The ε_c which was considered a measure of critical strain for the plastic relaxation increased with decreasing mean particle size.

Based on the observation of Bauschinger effect in many materials various theoretical models have been proposed to explain forward and reverse flow behaviour. The details of some basic models are discussed here.

1.5 THEORETICAL MODELS TO EXPLAIN BAUSCHINGER EFFECT

A number of macroscopic and microscopic models have been proposed (30) in order to explain the Bauschinger effect on metals. The macroscopic models are phenomenological in nature and are based on the continuum theory of plasticity. The microscopic approach aims to identify the hardening mechanisms and the magnitude of the internal stresses created within

the deforming material, the Bauschinger effect is a natural consequence of the unrelaxed internal stresses that are developed.

Macroscopic Models

(i) Model based on residual stresses

This model provides a rather crude interpretation of the effect of residual stresses upon the subsequent hardening behaviour. This model assumes that the residual stress distribution across the cross section of the cylindrical specimen as $\sigma = \sigma_o \cos \frac{\pi x}{t}$, where σ_o, t and x are fraction of initial yield, radii of the sample, and the distance from the tensile axis of the specimen respectively. It was observed that the reduction of the elastic limit and the rounding of the stress-strain curve is a function of σ_o. In this model no permanent softening is realized, unless a more accurate interpretation can be made of how the stresses were generated, not much more could be gained through the arbitrary selection of different stress distributions.

(ii) Hardening model using elastic-plastic elements [the Masing model (31)]

In this model the material is assumed to be composed of a number 'n' of elastic perfectly plastic elements of different yield strengths. Increasing the number of elements has the effect of rounding the stress-strain curve upto the point where the last element yields. If this model undergoes a cyclic loading then geometry of the flow curves in the forward

and reverse direction are identical apart from a scaling factor of 2.

In this model Bauschinger stress $\sigma_F - \sigma_R$ is always exhibited and is equal to $2(\sigma_F - \sigma_o)$ (twice the forward hardening) where σ_o is the initial yield. All the hardening comes from the back stress contribution. Permanent softening would not be exhibited with elastic perfectly plastic elements. On this basis, more sophisticated models also developed.

Microscopic Models

In the reference (32), it is proposed that following initial yielding the overall work hardening of the material comes from two main sources. One is forest hardening 'σ_{for}' arises due to dislocation interaction which is short range in nature. Secondly the particles give rise to an unrelaxed internal stress 'σ_M' in the matrix which aids the process of reverse flow which is long range in nature. The long range stresses are directional in nature and provide one of the hardening mechanisms during forward flow, but they also give rise to the Bauschinger effect exhibited during reverse flow. The predicted flow stress in the forward and reverse direction given by

$$\sigma_F = \sigma_o + \sigma_{for} + \sigma_M \qquad (1.1)$$

$$\sigma_R = \sigma_o + \sigma_{for} - \sigma_M \qquad (1.2)$$

where σ_F, σ_R and σ_o are forward, reverse and initial yield respectively.

Equation (1.1) and (1.2) gives

$$\Delta\sigma = 2\sigma_M$$

where $\Delta\sigma$ and σ_M are permanent softening obtained in the reverse flow and back stress respectively. Wilson and Konnen (33), and Wilson (21) studied the back stress using X-ray method. They observed the back stress was about one half the measured permanent softening for a number of materials.

1.6 SCOPE OF THE PRESENT INVESTIGATION

The present investigation is concerned with changes in mechanical properties of metals in terms of Bauschinger effect as a result of abrupt changes in the mode of mechanical testing from torsion to tension, tension to compression and torsion to reverse torsion at various prestrain values.

Several studies have been made on single crystals((1) to (6)) to understand the tensile flow behaviour of twisted samples. There have been relatively less number of studies dealing with torsional prestrain effects in the subsequent tensile behaviour of polycrystalline metals and alloys ((7) to (16)). It was observed that the initial flow stress and strain hardening rate are affected by the torsional prestrain. It was also found that if the torsional prestrain exceeded a certain value, the specimen failed in a brittle manner when subsequently loaded in tension. In order to explain this behaviour, two different interpretations have been suggested.

(i) Vaidya and Murty (14) have suggested that the increased rate of hardening in the initial region is due to the twist prestrain inhomogeneity from the inner to outer layers of a solid specimen.

(ii) On the other hand, Watson and Brown (15) proposed that the observed change in hardening rate is due to the Bauschinger effect. When the Bauschinger effect is large, its elimination by straining leads to a rapid increase in flow stress and a very high apparent strain hardening rate. The recent work by Rao and Murty (16) on mild steel, copper and aluminium shows that Bauschinger effect does not seems to play important role to understand the initial high work hardening rate of twisted specimen in the tensile behaviour. Due to the possibility of above two interpretations additional experiments are necessary to understand the above behaviour.

In the present investigation experiments were performed on mild steel (0.12% C), commercially pure copper and commercially pure aluminium metals to study the variation of mechanical behaviour as a function of Bauschinger effect, nature of prestrain and direction of testing. Since the Bauschinger effect is maximum in the reverse loading, the direct measurements of Bauschinger effect were made from tension to compression and torsion to reverse torsion tests. Combined effects of various tensile prestrains followed by fixed torsional prestrain were also studied using subsequent tension tests. Since a carburized

(i) Vaidya and Murty (14) have suggested that the increased rate of hardening in the initial region is due to the twist prestrain inhomogeneity from the inner to outer layers of a solid specimen.

(ii) On the other hand, Watson and Brown (15) proposed that the observed change in hardening rate is due to the Bauschinger effect. When the Bauschinger effect is large, its elimination by straining leads to a rapid increase in flow stress and a very high apparent strain hardening rate. The recent work by Rao and Murty (16) on mild steel, copper and aluminium shows that Bauschinger effect does not seems to play important role to understand the initial high work hardening rate of twisted specimen in the tensile behaviour. Due to the possibility of above two interpretations additional experiments are necessary to understand the above behaviour.

In the present investigation experiments were performed on mild steel (0.12% C), commercially pure copper and commercially pure aluminium metals to study the variation of mechanical behaviour as a function of Bauschinger effect, nature of prestrain and direction of testing. Since the Bauschinger effect is maximum in the reverse loading, the direct measurements of Bauschinger effect were made from tension to compression and torsion to reverse torsion tests. Combined effects of various tensile prestrains followed by fixed torsional prestrain were also studied using subsequent tension tests. Since a carburized

specimen shows a strength gradient across its section, some of the mild steel samples were carburized to various depths and tested in tension. The observed effects have been compared with a view to assess the role of the above two explanations suggested for the torsional prestrain effects.

CHAPTER 2

EXPERIMENTAL PROCEDURE

2.1 SPECIMEN PREPARATION

Specimens were machined from cylindrical rods of 1/2 inch diameter mild steel (0.13% C), copper and aluminium according to the dimensions shown in Figure 2. These machined specimens were suitably annealed so as to relieve the internal stresses. The details of annealing treatment are given below.

Machined mild steel specimens were first coated with an inorganic corrosion prevention coating and then heat treated at 700°C for 36 hours and furnace cooled. After heat treatment the surface coating on the specimen was removed by polishing with various grades of emery paper and also with diluted HNO_3. Finally specimens were washed, dried and subjected to various modes of mechanical tests.

Copper specimens were annealed in a vacuum sealed pyrex glass tube at 450°C for 24 hours. Aluminium specimens were annealed in air at 500°C for 24 hours. After heat treatment both copper and aluminium specimens were polished with emery paper.

Some of the annealed mild steel samples were carburised to various depths by heating them in charcoal at 920°C for 4 to 12 hours. After carburisation the specimens were air cooled and polished with emery paper.

2.2 MECHANICAL TESTING

(i) Torsion-Tension Test

In this test, specimens were first twisted to various amounts under torsion and then subsequently tested in tension. Both the torsion and tension tests were carried out in an Instron testing machine at a cross head speed of 0.2 mm/min (76°/min)in case of torsion and 0.5 mm/min in case of tension. These experiments were performed on Al, Cu and mild steel samples. The tensile tests were carried out using Extensiometer having 10% strain range. The tensile true strain and true stress were calculated using the following formulas

$$\text{Tensile true stress} = \frac{L}{A}(1 + \varepsilon_p)$$

$$\text{Tensile true strain} = \ln(1 + \varepsilon_p) + \sigma/E$$

where ε_p is engineering plastic strain, 'A' is initial area of cross section, L is load, E is the modulus of elasticity of the metal and σ is the true stress.

The Bauschinger effect terms in torsion-tension test were calculated in the following manner. Considering the nature of twist prestrain across the cross section of the sample the theoretical yield stress in the tensile direction of twisted samples can be calculated in two ways.

(i) The twist prestrain can be converted into an equivalent tensile prestrain by using the relation

$$\varepsilon_p = \frac{2\,R\theta}{3\sqrt{3}}$$

where R is the radius of the specimen and Θ is the angle of twist in Rad./mm. The tensile stress-strain behaviour of annealed sample is given by $\sigma = K \varepsilon^n$ where σ is the true stress value corresponding to a true strain ε, K is the strength coefficient and n is strain hardening exponent. By substituting tensile equivalent strain ε_p of twisted sample in the above equation we can get theoretical tensile yield stress, i.e.,

$$\sigma_t = K \left(\frac{2\,\Theta R}{3\sqrt{3}}\right)^n$$

(ii) The tensile prestrain of twisted samples shows variation between centre to perphery. It has minimum at centre and maximum at periphery and hence due to strain hardening the tensile flow stress of each annular region calculated by using above formula (i.e. $\sigma = K \varepsilon^n$ where ε is equivalent tensile prestrain) shows variation accordingly. So by integrating this calculated flow stress for each annular region over the area of cross section of twisted sample we can get theoretical tensile yield stress of twisted sample which was given by

$$\sigma_t = \frac{2K}{n+2} \left(\frac{\Theta}{\sqrt{3}}\right)^n R^n$$

where Θ is the angle of twist in Radian/mm, R is the radius of the specimen, K is the strength coefficient,

n is the strain hardening exponent and σ_t is the theoretical tensile yield stress.

The flow stress values calculated by the above two methods are found to be almost the same.

The difference between theoretical yield point and observed yield point in tension of twisted sample was calculated as Bauschinger stress.

The plastic strain required to attain the theoretical yield point or fixed fraction of theoretical yield point in tension of twisted sample was calculated as Bauschinger strain.

The energy saved to bring the flow stress to the theoretical value or to the fixed fraction of the theoretical value was calculated as Bauschinger energy.

(ii) Tension-Compression Test

In this test specimens were first prestrained in tension to some value and then load is reversed to compression upto 0.2% compressive strain value. Above cycle is repeated on the same specimen for various tensile strains. This tension-compression tests were carried out in MTS testing machine using diametral extensiometer. The system was operated under load control mode, Ramp-Ramp through zero signal and at a loading rate 10 Ton/300 sec. The true stress-strain values are calculated using the following formulas

Tensile true stress $S = L/A$

Tensile true strain $= 2\ln\left(\frac{d_o}{d}\right) + S/E$

$$\text{Compressive true strain} = 2\ln(d/d_o) + S/E$$

where L is the load, A is the area of cross section at any instant, d_o is the initial diameter, d is the diameter at any instant, S is the true stress at any instant and E is the modulus of elasticity of the metal.

(iii) Tension-Torsion-Tension Test

In this test, specimens were first prestrained in tension to various strain values and then subjected to the same angle of twist through a torsion test and tested finally tested in tension. These tests were carried out in an Instron testing machine at a cross head speed of 0.2 mm/min (76°/min) in case of torsion and 0.5 mm/min in case of tension. After tension-torsion test the total tensile prestrain was calculated by adding tensile prestrain and equivalent tensile prestrain corresponding to the given torsion. Then the theoretical tensile yield stress can be calculated by using the following formula

$$\sigma_t = K (\varepsilon_t)^n$$

where ε_t is the total tensile prestrain, K is strength coefficient and σ_t is the theoretical yield stress. Bauschinger effect terms were calculated by similar to torsion-tension test.

(iv) Torsion to Reverse Torsion Test

Torsion followed by reverse torsion tests were carried out in an Instron testing machine. First materials are twisted to a particular strain value in forward direction and then

reversed upto 2% maximum shear strain value. This cycle is repeated for different forward torsional strain values. From the torque versus angle of twist curve maximum shear stress versus maximum shear strain were plotted using the following formulas

$$\text{Maximum shear strain} = \theta R$$

$$\text{Maximum shear stress} = \frac{1}{2\pi R^3}\left(3T + \theta \frac{dT}{d\theta}\right)$$

where θ is the angle of twist in Radian/mm, 'T' is the torque in kg-mm, $\frac{dT}{d\theta}$ is the slope of T-θ curve, and R is the radius of the sample. Bauschinger effect terms are calculated similar to tension-compression test.

CHAPTER 3

RESULTS

3.1 TORSION-TENSION TEST

(i) Mild steel (0.13% C), copper and aluminium samples were twisted to various prestrain levels and subsequently tested in tension. The details of these results are as follows. The tensile behaviour of twisted specimens of mild steel, copper and aluminium are shown in Figures 3 , 4 and 5 respectively. It can be noted from these figures that yield point, work-hardening rate and ultimate tensile strength in the tensile test are increased by increasing the twist prestrain, whereas the ductility and reduction in area decreased with twist prestrain (Table I). In all the above materials, the initial linear high work-hardening range of twisted specimen in tensile test was extended upto ≈ 0.05% strain level. The initial linear high work-hardening rate of twisted specimens in tensile test varied from 0.2 E to 0.6 E depending upon twist prestrain value (E is the modulus of elasticity of the material). Work-hardening rates of twisted mild steel (Figure 3), copper (Figure 4) and aluminium (Figure 5) at various offset values are given in Tables II, IIIa and IV respectively.

(ii) In torsion-tension tests, the Bauschinger effect factors were measured indirectly. The details of calculation

involved in measurement of Bauschinger effect parameters in torsion-tension test are given in the previous chapter under Experimental Procedure.

The calculated Bauschinger effect factors in mild steel, copper and aluminium for various twist prestrains are given in Tables V, VI and VII respectively. The variation of Bauschinger stress, Bauschinger strain and Bauschinger energy with tensile equivalent prestrain are plotted for mild steel (Figures 6, 7 and 8) and copper (Figures 9 and 10). It is seen that Bauschinger effect increases with twist prestrain.

Variation of Bauschinger factors with work-hardening rate for mild steel (Figures 11 and 12) and copper (Figures 13 and 14) were plotted. For lower Bauschinger effect (Bauschinger stress $\leq$ 240 MPa in case of copper, $\leq$ 120 MPa in case of mild steel) the work-hardening rate is strongly dependent on Bauschinger effect, but at higher Bauschinger effect, the work-hardening rate is almost independent of Bauschinger effect.

3.2 TENSION-COMPRESSION TESTS

(i) In order to make direct measurement of Bauschinger effect, tension-compression tests were conducted on mild steel (Figure 15) and copper (Figure 16). The observations made on mild steel are given in Tables VIII and IX. It was observed that in mild steel, the yield point in the compressive direction increases with tensile prestrain, whereas work-hardening rate in the compressive direction does not show any change with

tensile prestrain. In the case of copper, it can be noted from Table X that the yield point and work-hardening rate in compressive direction increased with tensile prestrain.

(ii) The values of Bauschinger factors at various prestrain levels for mild steel and copper are shown in Tables IX and XI respectively. Tables IX and XI show that Bauschinger stress, Bauschinger strain and Bauschinger energy increase with tensile prestrain. Variation of Bauschinger factors (Bauschinger stress, Bauschinger strain and Bauschinger energy) with prestrain for mild steel is plotted in Figures 6, 7 and 8 and for copper in Figures 9 and 10.

Plots of the work-hardening rate with Bauschinger factors for mild steel (Figures 11 and 12) and copper (Figures 13 and 14) show that in the case of mild steel the work-hardening rate is independent of Bauschinger effect, but in the case of copper the work-hardening rate increases with Bauschinger factors.

3.3 COMPARATIVE STUDY OF TORSION-TENSION AND TENSION-COMPRESSION TESTS

In order to understand the correlation between the Bauschinger effect and the twist prestrain effect, comparison between tension-compression and torsion-tension test data is essential.

(i) It was observed that both the materials show increase in Bauschinger effect (Bauschinger stress, Bauschinger strain and Bauschinger energy) with prestrain in tension-compression and torsion-tension tests. Observations made on mild steel (Figures 6, 7 and 8) and copper (Figures 9 and 10)

show that for the same tensile equivalent prestrain or tensile prestrain value, torsion-tension test shows lesser Bauschinger effect than the tension-compression test.

(ii) Variations of work-hardening rate with Bauschinger stress in torsion-tension and tension-compression tests for mild steel and copper are plotted in Figures 11 and 12 and in Figures 13 and 14 respectively. It is seen that for the same Bauschinger effect (Bauschinger stress or Bauschinger strain or Bauschinger energy) torsion-tension tests show higher work-hardening rate (1.5 to 2 times in case of Bauschinger stress) than that of tension-compression test.

3.4 TORSION-REVERSE TORSION TEST

Torsion followed by reverse torsion test is another method of measuring Bauschinger factors directly in terms of maximum shear stress and maximum shear strain. This test has been conducted to study the variation of work-hardening rate with Bauschinger effect and the prestrain dependency of Bauschinger effect.

(i) Maximum shear strain versus maximum shear stress for mild steel and copper are shown in Figures 17 and 18 respectively. The observation made on mild steel and copper are given in Tables XII and XIII respectively. From these tables it can be noted that the Bauschinger effect (Bauschinger stress, Bauschinger strain and Bauschinger energy) increases with torsional prestrain.

(ii) The Tables XII and XIII show that in both the materials the work-hardening rate has a value of about 0.3 G (G is the rigidity modulus of the material) and it is independent of prestrain value and magnitude of Bauschinger effect (Bauschinger stress, Bauschinger strain and Bauschinger energy).

3.5 TENSION-TORSION-TENSION TEST

Combined effects of various tensile prestrains followed by fixed torsional prestrain were studied using subsequent tension test which is denoted here as tension-torsion-tension test. In this test Bauschinger effect factors were measured indirectly. This kind of tests were performed on mild steel samples and its tensile behaviour is shown in Figure 19. The observations made from this figure are given in the Table XIV.

(i) Figure 19 shows that the yield point and ultimate tensile strength increase with tensile prestrain.

(ii) From Table XIV, it is seen that the Bauschinger effect decreases with increasing tensile prestrain. Variation of Bauschinger stress, Bauschinger strain and Bauschinger energy with total tensile equivalent prestrain are plotted in Figures 6, 7 and 8 respectively.

(iii) Work-hardening rate in the tensile test did not change with tensile prestrain as well as the magnitude of Bauschinger effect.

3.6 SPECIMEN DIAMETER EFFECT IN TORSION-TENSION TESTS

The tensile stress-strain curves of twisted copper samples of various diameter (4 mm and 6.5 mm) are given in Figures 20 and 21. Variation of Bauschinger effect with prestrain is given in Table VI and in Figures 9 and 10.

(i) From Figures 9 and 10 it can be seen that for same equivalent tensile prestrain the specimens of diameter 6.5 mm show larger Bauschinger effect in comparison to 4 mm diameter specimens.

(ii) Variation of work-hardening rate with Bauschinger stress for samples of various diameter is shown in Figure 13. It was observed from the Figure 13 that for the same Bauschinger stress specimens of bigger diameter (6.5 mm) shows higher initial work-hardening rate (0.001 offset value) than that of specimens of smaller dimension (4 mm). It can be seen from the table that specimens of bigger diameter (6.5 mm) do not show any variation in work-hardening rate with Bauschinger effect.

3.7 TENSILE TESTS ON CARBURISED MILD STEEL SAMPLES

Tests of carburised mild steel samples were performed to study the effect of strength gradient across the cross section of the sample on the tensile behaviour. The tensile stress-strain curves of mild steel samples carburised to various depths (0.5 mm, 1 mm and 2 mm) are shown in Figure 22. The data from Figure 22 are given in Table XV.

(i) From Figure 22 it can be seen that the yield point, UTS and initial work-hardening rate are all increased by increasing depth of carburisation.

(ii) The work-hardening rate at various offset strain values are plotted and compared with torsion-tension test (Figure 23). The initial work-hardening rate of carburised samples in the tensile tests is in the range of 0.3 E to 0.6 E which is comparable with that of work-hardening rate of twisted samples in the tensile test.

(iii) It can be seen from Figure 22 that the initial linear high work-hardening range is extended upto $\sim$ 0.05% strain value.

CHAPTER 4

DISCUSSION

From the tensile tests of twisted samples, it is found that torsional prestrain raises the UTS and lowers the percent reduction in area and elongation. These observations are similar to those reported by Swift (7). In addition to the above, the observations made by Vaidya and Murty (14) on copper and the observation made by Rao and Murty (16) on mild steel, copper and aluminium in torsion-tension test show that the initial high work-hardening rate region observed in tension following torsion has a slope of about 0.06 E and it extends upto 2% strain value, where E is the modulus of elasticity of the material. But the present study on mild steel, copper and aluminium show that the initial linear region has a maximum slope of about 0.6 E and it extends upto $\sim$ 0.05% strain value. These observations are similar to those reported by Watson and Brown (15). In the present case, experiments were performed with extensometer mounted on the tensile specimen.

Tensile tests were also carried out on twisted aluminium in order to compare the results with and without extensometer on the sample and these data are shown in Figure 24. Samples tested without extensometer show initial linear work-hardening rate upto a maximum value of about 0.2 E and this region of high work-hardening rate extends upto $\sim$ 1% strain value. Thus

the data without extensometer on the sample seems to be error.

There are two kinds of interpretation for explaining the above phenomenon.

(i) One is "strain inhomogeneity theory" suggested by Vaidya and Murty (14).

(ii) Secondly, the above phenomenon is explained in terms of Bauschinger effect by Watson and Brown (15).

The results of present investigation can now be considered in assessing the above two interpretations. All the materials in torsion-tension tests show that Bauschinger effect increases with prestrain value. Similar kind of relationship is shown by mild steel (Table IX) and copper (Table XI) in tension-compression tests.

Comparative study of torsion-tension and tension-compression tests show that for the same tensile equivalent prestrain or tensile prestrain value, torsion-tension test shows lesser Bauschinger effect than tension-compression test. It is seen that for the same Bauschinger effect torsion-tension test shows higher work-hardening rate (1.5 to 2 times for the same Bauschinger stress) than that of tension-compression test (Figures 11 to 14).

The results on torsion-reverse-torsion tests show that while Bauschinger effect increases with prestrain value, the initial work hardening rate is independent of prestrain value and magnitude of Bauschinger effect.

In case of tension-torsion-tension test, variation of Bauschinger effect with equivalent tensile prestrain on mild

steel is shown in Figure 19. In this test it is observed that Bauschinger effect decreases by increasing tensile prestrain. From Table XIV it can be seen that in tension-torsion-tension tests the work-hardening rate does not vary with the magnitude of Bauschinger effect.

All the above results are incompatible with the interpretation given by Watson and Brown (15). From these results it is obvious that there is no definite relation between work-hardening rate and Bauschinger effect. Thus, Bauschinger effect does not seem to play an important role in the high initial work-hardening rate shown by twisted samples in tension.

The results of torsion-tension test on copper of various diameter show that the initial work-hardening rate of twisted samples of bigger diameter (6.5 mm) has a value of about 0.55 E and does not show any variation with Bauschinger effect. From the Figure 13 it can be seen that for the same Bauschinger stress samples of bigger diameter (6.5 mm) exhibit higher work-hardening rate (at 0.001 offset strain value) than that of specimens of smaller diameter (4 mm).

As we increase the diameter of samples for the same twist prestrain value the strain inhomogeneity is expected to increase. Similar kind of observations were also made by Rao and Murty (16) on copper, aluminium and mild steel samples. Further it was observed that the microhardness of the twisted samples varies along the diameter of a twisted specimen. The hardness was minimum in core region (~ 170 DPH in case of 4 mm diameter mild steel sample twisted to 0.2339 Radians/min) and

maximum (225 DPH) at the case region. In the present work, the hardness data on 6 mm diameter mild steel specimens twisted to 0.649 Radians/mm are shown in Figure 25. It can be seen that there is no systematic variation of hardness value along the diameter of twisted specimen.

The tensile tests on carburised mild steel samples also support the strain inhomogeneity theory. The work hardening rates of carburised samples in tensile tests are comparable with those of twisted samples in tensile test as shown in Figures 22 and 23. The yield stress and work-hardening rate of carburised samples are observed to increase by increasing depth of carburisation. In the case of carburised samples the case region is having a higher yield than the soft core region, as shown by microhardness measurement (Figure 26). The minimum hardness value at core region is $\sim$ 150 DPH, whereas the maximum value is $\simeq$ 400 DPH at the case region in case of carburised sample to 1 mm depth. Thus when we subject carburised mild steel specimens to tension, the core region yields first and rapid dislocation multiplication will take place until its strength reaches that of case region, thereby resulting in a very high work-hardening rate initially.

CHAPTER 5

CONCLUSIONS

(i) The initial work-hardening rate in tension of twisted mild steel, copper and aluminium is considerably high (varies from 0.2 E to 0.6 E where E is the modulus of elasticity of the material) and it increases with increasing prestrain. This linear work-hardening range extends upto 0.05% strain value.

(ii) The initial rate of work-hardening in the stress reversal tests (tension-compression, tension to reverse torsion) is smaller than the corresponding values in torsion-tension tests.

(iii) Comparison of the work-hardening rate of torsion-tension and tension-compression test for the same Bauschinger effect shows that torsion-tension test yields higher work-hardening rate than the tension-compression test.

(iv) Combined effects of various tensile prestrain followed by fixed torsional prestrain on subsequent tensile test also confirm that the initial work-hardening rate is independent of the magnitude of Bauschinger effect.

(v) From (iii) and (iv) it is obvious that the correlation between Bauschinger effect and work-hardening rate is not in conformity with the interpretation that the

initial high work-hardening rate is a consequence of Bauschinger effect in torsion-tension test.

(vi) Tensile tests on mild steel specimens carburised to different depths indicate a region of high work-hardening rate similar to that of torsion-tension tests.

TABLE I : Torsion-Tension Test

Material and dimension	Amount of twist θ Radians/mm	True stress at maximum load MPa	Percentage elongation $\frac{\Delta l}{l_o} \times 100$	Percentage reduction in area $\frac{\Delta A}{A} \times 100$	K MPa	n
Mild steel 6 mm diameter	0	336.08	19.8	16.5		
	0.06816	326.12	10.2	9.3		
	0.1424	367.50	1.8	1.7	545.51	0.2864
	0.215	393.75	0.6	0.6		
	0.5918	419.27	0.08	0.08		
Copper 6.5 mm diameter	0	270.51	28.2	22.0		
	0.1494	251.86	9.8	8.9		
	0.3029	281.30	1.7	1.7	495.63	0.4545
	0.8805	340.82	1.53	1.5		
	1.2249	363.80	1.1	1.1		
Aluminium 6.4 mm diameter	0	106.14	20.8	17.0		
	0.1554	122.25	0.8	0.8	142.89	0.1806
	0.4232	151.86	0.68	0.68		
	0.6985	172.08	0.3	0.3		

NOTE: K is strength coefficient; Δl corresponds to the extension till UTS value; n is strain-hardening exponent; ΔA corresponds to the change in area till UTS value.

TABLE II : Torsion-Tension Tests on 6 mm Diameter Mild Steel Samples

θ Radians/mm	Equivalent average tensile prestrain ε_{eq}	Calculated yield point in tension σ_c		Observed yield point in tension, MPa	
		$K(\varepsilon_{eq})^n$ MPa	$\frac{2K(R\,\theta/\sqrt{3})^n}{2+n}$ MPa	Deviation from linearity	0.005 offset value
0	-	-	-	48.14	80
0.06816	0.081	265.64	260.98	170.24	228
0.1424	0.1644	325.28	319.57	204.46	304
0.2150	0.2462	365.14	358.74	242.57	352
0.5918	0.6890	490.32	481.71	308.35	404

θ Radians/mm	Work-hardening rate in terms of modulus of elasticity of steels at various offset strain values							
	0.00025	0.0005	0.00075	0.0012	0.002	0.003	0.005	0.01
0	0.227	0.155	0.097	0.092	0.048	0.023	0.019	0.012
0.06816	0.276	0.121	0.102	0.076	0.052	0.034	0.019	0.01
0.1424	0.387	0.242	0.138	0.081	0.046	0.032	0.016	0.005
0.2150	0.352	0.258	0.176	0.143	0.046	0.036	0.011	-
0.5918	0.446	0.297	0.227	-	-	-	-	-

TABLE IIIa : Torsion-Tension Test on 4 mm Diameter Copper Samples

θ Radians/mm	Equivalent average tensile prestrain ε_{eq}	Calculated yield point σ_c MPa		Observed yield point MPa	
		$\frac{2K(R\,\theta/\sqrt{3})^n}{2+n}$	$K(\varepsilon_{eq})^n$	Deviation from linearity	0.001 offset value
0	-	-	-	26.84	40
0.1653	0.1263	189.59	193.52	42.81	144
0.3191	0.2456	256.54	261.85	49.83	190
0.83	0.6389	396.13	404.33	69.01	224
1.1607	0.8935	461.35	470.90	71.31	228
1.6822	1.2950	546.11	557.41	80.51	264

θ Radians/mm	Work-hardening rate at various offset strain values in terms of modulus of elasticity of copper					
	0.0005	0.001	0.002	0.003	0.004	0.006
0	0.02	0.02	0.02	0.02	0.02	0.02
0.1653	0.403	0.363	0.242	0.107	0.038	0.01
0.3191	0.558	0.29	0.165	0.081	0.048	0.01
0.83	0.518	0.403	0.201	0.107	0.074	0.01
1.1607	0.605	0.363	0.201	0.125	0.101	0.05
1.6822	0.605	0.403	0.242	0.125	0.101	-

TABLE IV : Torsion-Tension Test on 6.4 mm Diameter Aluminium Samples

Extensometer	θ Rad./mm	Equivalent tensile prestrain ε_{eq}	Calculated yield point σ_c MPa		Observed yield point MPa	
			$\frac{2K(R\theta/\sqrt{3})^n}{n+2}$	$K(\varepsilon_{eq})^n$	Deviation from linearity	0.001 offset value
Tests with Extensometer	0	-	-	-	22.26	31
	0.1554	0.1914	104.61	106.00	56.91	106
	0.4232	0.5131	125.00	126.67	61.82	115
	0.6985	0.8469	136.84	138.67	68.00	152.5
Tests without Extensometer	0.9943	1.6513	145.26	147.20	46.88	58
	0.5159	1.1787	130.51	132.24	37.05	45

Extensometer	θ Rad./mm	Work-hardening rate in terms of modulus of elasticity at various offset strain values				
		0.0005	0.001	0.002	0.003	0.005
Tests with Extensometer	0	0.098	0.068	0.045	0.045	0.03
	0.1554	0.363	0.201	0.077	0.04	0.01
	0.4232	0.426	0.279	0.18	0.08	0.03
	0.6985	0.558	0.213	0.13	0.07	-
Tests without Extensometer	0.9943	0.173	0.173	0.173	0.173	0.13
	0.5159	0.110	0.110	0.110	0.110	0.11

TABLE V : Torsion-Tension Tests on Mild Steel Samples

θ Radians/mm	Equivalent tensile prestrain	$\Delta\sigma$ MPa	$\Delta\sigma_{0.0005}$ MPa	$\beta_{0.75\,\sigma_c}$	E_s $\times 10^6$ Joules/m^3
0	-	-	-	-	-
0.06816	0.081	90.74	32.98	0.0001	0.0012
0.1424	0.1644	115.11	15.57	0.00013	0.0018
0.215	0.2462	116.17	26.74	0.00009	0.0004
0.5918	0.6890	172.86	77.71	0.00025	0.004

TABLE VI : Torsion-Tension Tests on Copper Samples

Diameter	θ Rad./mm	Equivalent tensile prestrain ε_{eq}	$\Delta\sigma$ MPa	$\Delta\sigma_{0.001}$ MPa	$\beta_{0.6\sigma_c}$	$E_{s(0.6\,\sigma_c)}$ $\times 10^6$ Joules/m^3
4 mm	0.1653	0.1263	146.78	45.59	0.0005	0.016
	0.3191	0.2456	206.54	46.54	0.00056	0.02
	0.83	0.6389	327.12	172.13	0.0012	0.074
	1.1607	0.8935	390.04	233.35	0.0022	0.1432
	1.6822	1.2950	465.60	282.11	0.003	0.2
6.5 mm	0.1494	0.2027	195.59	117.08	0.0007	0.03
	0.3029	0.4063	274.48	126.46	0.001	0.06
	0.8805	1.1116	435.38	285.50	0.0039	0.21
	1.2249	1.5464	460.85	343.98	0.0087	0.384

TABLE V : Torsion-Tension Tests on Mild Steel Samples

θ Radians/mm	Equivalent tensile prestrain	$\Delta\sigma$ MPa	$\Delta\sigma_{0.0005}$ MPa	$\beta_{0.75\ \sigma_c}$	E_s $\times 10^6$ Joules/m^3
0	-	-	-	-	-
0.06816	0.081	90.74	32.98	0.0001	0.0012
0.1424	0.1644	115.11	15.57	0.00013	0.0018
0.215	0.2462	116.17	26.74	0.00009	0.0004
0.5918	0.6890	172.86	77.71	0.00025	0.004

TABLE VI : Torsion-Tension Tests on Copper Samples

Diameter	θ Rad./mm	Equivalent tensile prestrain ε_{eq}	$\Delta\sigma$ MPa	$\Delta\sigma_{0.001}$ MPa	$\beta_{0.6\sigma_c}$	$E_{s(0.6\ \sigma_c)}$ $\times 10^6$ Joules/m^3
4 mm	0.1653	0.1263	146.78	45.59	0.0005	0.016
	0.3191	0.2456	206.54	46.54	0.00056	0.02
	0.83	0.6389	327.12	172.13	0.0012	0.074
	1.1607	0.8935	390.04	233.35	0.0022	0.1432
	1.6822	1.2950	465.60	282.11	0.003	0.2
6.5 mm	0.1494	0.2027	195.59	117.08	0.0007	0.03
	0.3029	0.4063	274.48	126.46	0.001	0.06
	0.8805	1.1116	435.38	285.50	0.0039	0.21
	1.2249	1.5464	460.85	343.98	0.0087	0.384

TABLE VII : Torsion-Tension Tests on 6.4 mm Diameter Aluminium Sample

Extensiometer	θ Radians/mm	Equivalent tensile prestrain ε_{eq}	$\Delta\sigma$ MPa	β MPa	E_s $\times 10^6$ Joules/m^3
Tests with Extensiometer	0.1554	0.1914	47.70	0.0007	0.0133
	0.4232	0.5131	63.18	0.0014	0.0315
	0.6985	0.8469	68.84	0.0006	0.0155
Tests without Extensiometer	0.9943	1.1787	98.38	0.0096	0.3125
	0.5159	0.6513	93.46	0.0152	0.5500

TABLE VIII : Tension-Compression Tests on Annealed Mild Steel Sample

Cycle	Tensile prestrain	Stress at the point of unloading in tension σ_u MPa	Compressive yield MPa	
			Deviation from linearity	0.001 offset value
Ist	0.0152	172.98	49.39	122
IInd	0.0477	236.98	95.60	144
IIIrd	0.0972	291.86	100.48	176
IVth	0.1959	359.64	140.50	202

Cycle	Tensile prestrain	Work-hardening rate in terms of modulus of elasticity of steel incompressive direction at various offset values			
		0.00025	0.00075	0.001	0.0075
Ist	0.0152	0.276	0.175	0.129	0.092
IInd	0.0477	0.193	0.175	0.161	0.121
IIIrd	0.0972	0.242	0.193	0.161	0.138
IVth	0.1959	0.242	0.193	0.176	0.129

TABLE IX : Tension-Compression Tests on Mild Steel

Cycle	Tensile prestrain	$\Delta\sigma$ MPa	$\Delta\sigma_{0.001}$	$\beta_{0.75\ \sigma_u}$	$E_{s_{0.75\sigma_u}}$ x10^6 Joules/m^3
Ist	0.0152	123.59	50.98	0.00125	0.0348
IInd	0.0477	144.38	92.98	0.002	0.068
IIIrd	0.0972	191.38	115.86	0.0022	0.094
IVth	0.1959	219.14	157.64	0.0032	0.169

TABLE X : Tension-Compression Tests on 6 mm Diameter Copper Samples

Cycle	Tensile prestrain value	Stress at the point of unloading in tension σ_u MPa	Compressive yield MPa	
			Deviation from linearity	0.001 off-set value
Ist	0.0021	42.70	18.78	38
IInd	0.0524	127.56	30.51	80
IIIrd	0.1052	183.72	35.95	102
IVth	0.1595	226.13	39.95	128
Vth	0.2232	264.75	44.14	144

Cycle	Tensile prestrain value	Work-hardening rate at various offset strain values in terms of modulus of elasticity of copper			
		0.0005	0.001	0.0015	0.002
Ist	0.0021	0.14	0.12	0.09	0.076
IInd	0.0524	0.3	0.191	0.15	0.121
IIIrd	0.1052	0.363	0.259	0.21	0.165
IVth	0.1595	0.453	0.279	0.227	0.201
Vth	0.2232	0.453	0.330	0.242	0.227

TABLE XI : Tension-Compression Tests on Copper Sample

Cycle	Tensile prestrain	$\Delta\sigma$ MPa	$\Delta\sigma_{0.001}$ MPa	$\beta_{0.6\,\sigma_u}$	$E_{s(0.6\,\sigma_u)} \times 10^6$ Joules/m^3
Ist	0.0021	23.92	4.70	0.0002	0.00065
IInd	0.0524	97.05	47.56	0.0009	0.017
IIIrd	0.1052	147.77	81.72	0.0012	0.037
IVth	0.1595	186.18	98.13	0.0012	0.0455
Vth	0.2232	220.61	120.75	0.0015	0.06

TABLE XII : Torsion-Reverse-Torsion Tests on 6 mm Diameter Mild Steel Sample

Cycle	Maximum shear strain in forward torsion	Maximum shear stress at the point of reversal in forward torsion σ_F MPa	Yield stress in the reverse torsion. Deviation from linearity MPa	$\Delta\sigma$ MPa	$\beta_{0.6\ \sigma_F}$	$E_{s(0.6\ \sigma_F)}$ $\times 10^6$ Joules/m^3
Ist	0.4329	193.32	43.03	150.29	0.002	0.044
IInd	0.8817	223.52	45.44	178.08	0.003	0.108
IIIrd	1.3215	239.48	51.74	187.74	0.0032	0.120

Cycle	Maximum shear strain in forward torsion	Work-hardening rate at various offset strain values in terms of rigidity modulus			
		0.001	0.002	0.004	0.005
Ist	0.4329	0.183	0.139	0.081	0.061
IInd	0.8817	0.249	0.183	0.081	0.061
IIIrd	1.3215	0.244	0.183	0.081	0.07

TABLE XIII : Torsion-Reverse-Torsion Test on 6.5 mm Diameter Copper Sample

Cycle	Maximum shear strain in forward torsion	Maximum yield shear stress at the point of reversal in the forward torsion 'σ_F' MPa	Yield stress in the reverse torsion. Point of deviation from linearity MPa	$\Delta\sigma$ MPa	$\beta_{0.75\ \sigma_F}$	$E_{s(0.75\ \sigma_F)}$ $\times 10^6$ Joules/m^3
Ist	0.639	143.45	25.08	118.41	0.0075	0.176
IInd	1.2555	158.28	32.26	126.02	0.0075	0.182
IIIrd	1.8834	167.47	36.18	131.29	0.0085	0.216

Cycle	Maximum shear strain in the forward torsion	Work-hardening rate in terms of rigidity modulus at various offset strain values			
		0.001	0.003	0.005	0.007
Ist	0.639	0.24	0.161	0.09	0.066
IInd	1.2555	0.18	0.145	0.096	0.048
IIIrd	1.8884	0.30	0.145	0.096	0.0603

TABLE XIV : Tension-Torsion-Tension Tests on 6 mm Diameter Mild Steel Samples

Tensile prestrain	Angle of twist θ Radians/mm	Total prestrain ε_t	Theoretical yield point $K(\varepsilon_t)^n$	Observed yield point	
				Point of deviation from linearity	0.0005 offset value
0.0294	0.2937	0.3382	399.91	176.95	296
0.0665	0.2818	0.3648	405.68	251.44	354
0.1190	0.2818	0.4059	418.27	298.10	494

Total prestrain	$\Delta\sigma$	$\Delta\sigma_{0.0005}$	β	E_s $x10^6$ Joules/m^3	*Work-hardening rate at various offset strain values in terms of modulus of elasticity of steel*		
					0.00025	0.0005	0.001
0.3382	222.96	103.91	0.0051	0.1688	0.483	0.463	0.215
0.3648	154.24	51.68	0.0042	0.0644	0.483	0.258	0.193
0.4059	120.17	25.00	0.0014	0.028	0.483	0.480	0.161

TABLE XV : Tensile Test of Carburised 6 mm Diameter Mild Steel Samples

Depth of carburisation	Yield point		Work-hardening rate in terms of modulus of elasticity of mild steel at various offset strain values						
	Deviation from linearity MPa	0.001 offset value MPa	0.00025	0.0005	0.00075	0.0012	0.002	0.003	0.005
0.5 mm	210.00	300	0.352	0.276	0.168	0.077	0.051	0.028	0.028
1.0 mm	230.00	356	0.483	0.389	0.242	0.227	0.114	0.097	0.051
2.0 mm	278.01	448	0.604	0.387	0.258	0.190	0.114	0.097	0.051

REFERENCES

1. Paxton H.W. and Cottrell A.H., Acta Metall. 2, 3 (1954).
2. Rebstock H., Z. Metallk. 48, 206 (1957).
3. Holt, D.B., Acta Metall. 7, 446 (1959).
4. Basinski Z.S. and Basinski S.J., Phil. Mag. 9, 51 (1964).
5. Osborne P.W., Acta Metall. 12, 747 (1964).
6. Paterson M.S., Acta Metall. 3, 491 (1955).
7. Swift H.W., JISI, 140, 181 (1939).
8. Korber F., Mih, K.W.I., 23, No. 123 (1941).
9. Hollowman J.H., Trans. AIME 158, 283 (1944).
10. Mehinger F.J., Trans. AIME 162, 291 (1945).
11. Lynch J.J., Trans. AIME 175, 435 (1948).
12. Fanpel J.H. and Marion J., ASM 36, 30.
13. Bridgeman, Studies in Large Plastic Flow and Fracture (McGraw Hill, New York), (1952).
14. Vaidya M.L. and Murty G.S., Scripta Met. 3, 263 (1969).
15. Watson J.D. and Brown G.G., Scripta Met. 7, 739 (1973).
16. Rao M.K. and Murty G.S., M.K. Rao's M.Tech. Thesis Work, Submitted in January 1978, I.I.T., Kanpur.
17. Bauschinger J., Zivilingur, Vol. 27, p. 287 (1881).
18. Abel A. and Muir H., Phil. Mag. 26, 489 (1972).
19. Ibrahim N. and Embury J.D., Mater. Sci. Eng., 19, 147 (1975).
20. Orowan E. in Internal Stresses and Fatigue of Metals, p. 59, ed., Rassweiler and Grube, Amsterdam, Elsevier (1966).
21. Wilson D.V., Acta Met. 13, 807 (1965).
22. Takao Yakov et al., Trans. of the JIM, Vol. 18, No. 1, (1977).

23. Buckley and Entwistle K.M., Acta Met. 4, 325 (1956).

24. Holley R.L., Phil. Mag., Vol. 44, 597 (1953).

25. Kishi T. and Gokyu I., Met. Trans., Vol. 4, 391 (1973).

26. Gupta S.P. and Kodali S.P., Scripta Metall., Vol. 10, 111 (1976).

27. Abel A. and Ham R.K., Acta Met., Vol. 14, 1489 (1966).

28. Stoltz R.F. and Pellows R.M., Metall. Trans., Vol. 7A, 1295 (Sep. 1976).

29. Matsuura et al., Trans. JIM, Vol. 20, No. 3, (March 1979).

30. Sowerby R. et al., Mat. Sci. Eng., 41, 43-58 (1979).

31. G. Masing, Wiss. Veröff. Siemens-Werken, 3, 321 (1923).

32. Brown L.M. and Stobbs W.M., Philos. Mag. 34, 351 (1976).

33. Wilson D.V. and Konnan Y.A., Acta Metall. 12, 617 (1964).

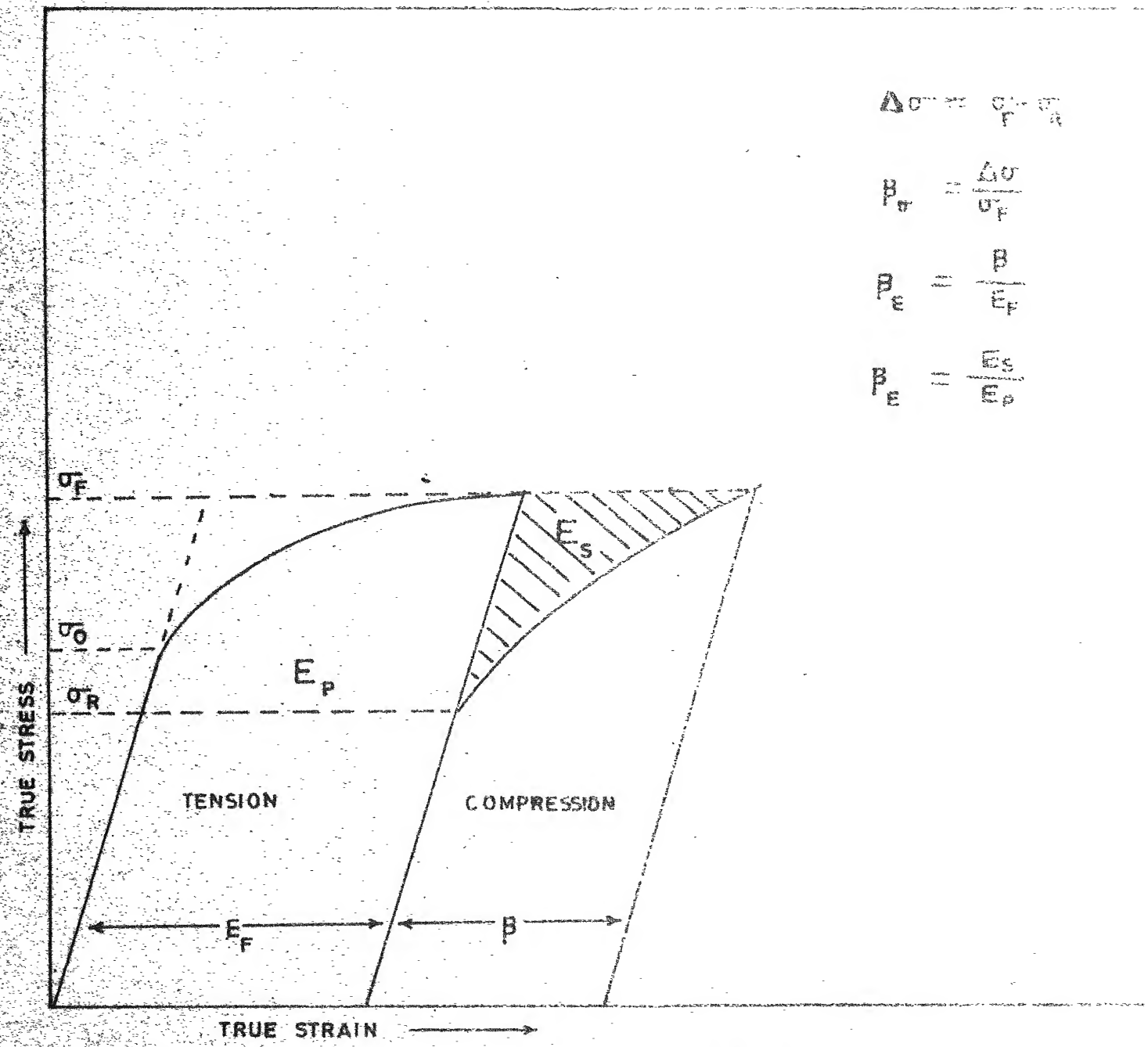

$$\Delta\sigma = \sigma_F - \sigma_R$$

$$\beta_\sigma = \frac{\Delta\sigma}{\sigma_F}$$

$$\beta_\varepsilon = \frac{\beta}{E_P}$$

$$\beta_E = \frac{E_S}{E_P}$$

FIG. 1

SPECIMEN DIMENSION

ALL DIMENSIONS ARE IN mm

TORSION TENSION TEST SPECIMEN

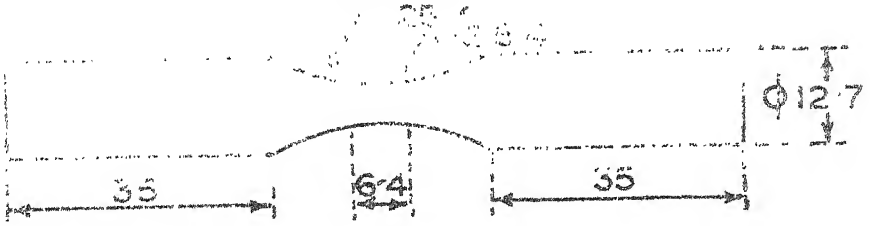

TORSION TENSION TEST SPECIMEN

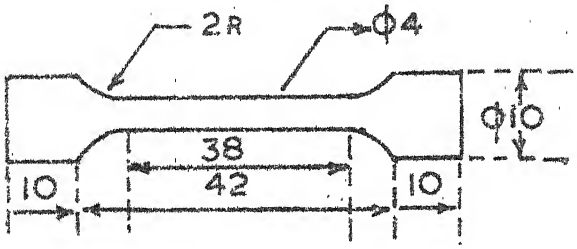

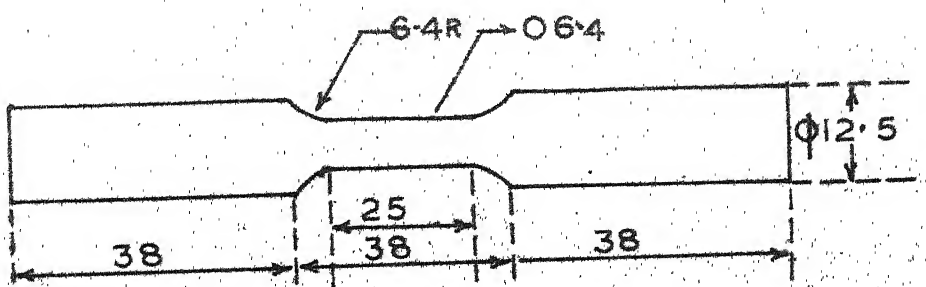

FIG. 2

TENSILE TESTS OF 6mm DIAMETER M.S SPECIMENS TWISTED TO VARIOUS ANGLES.

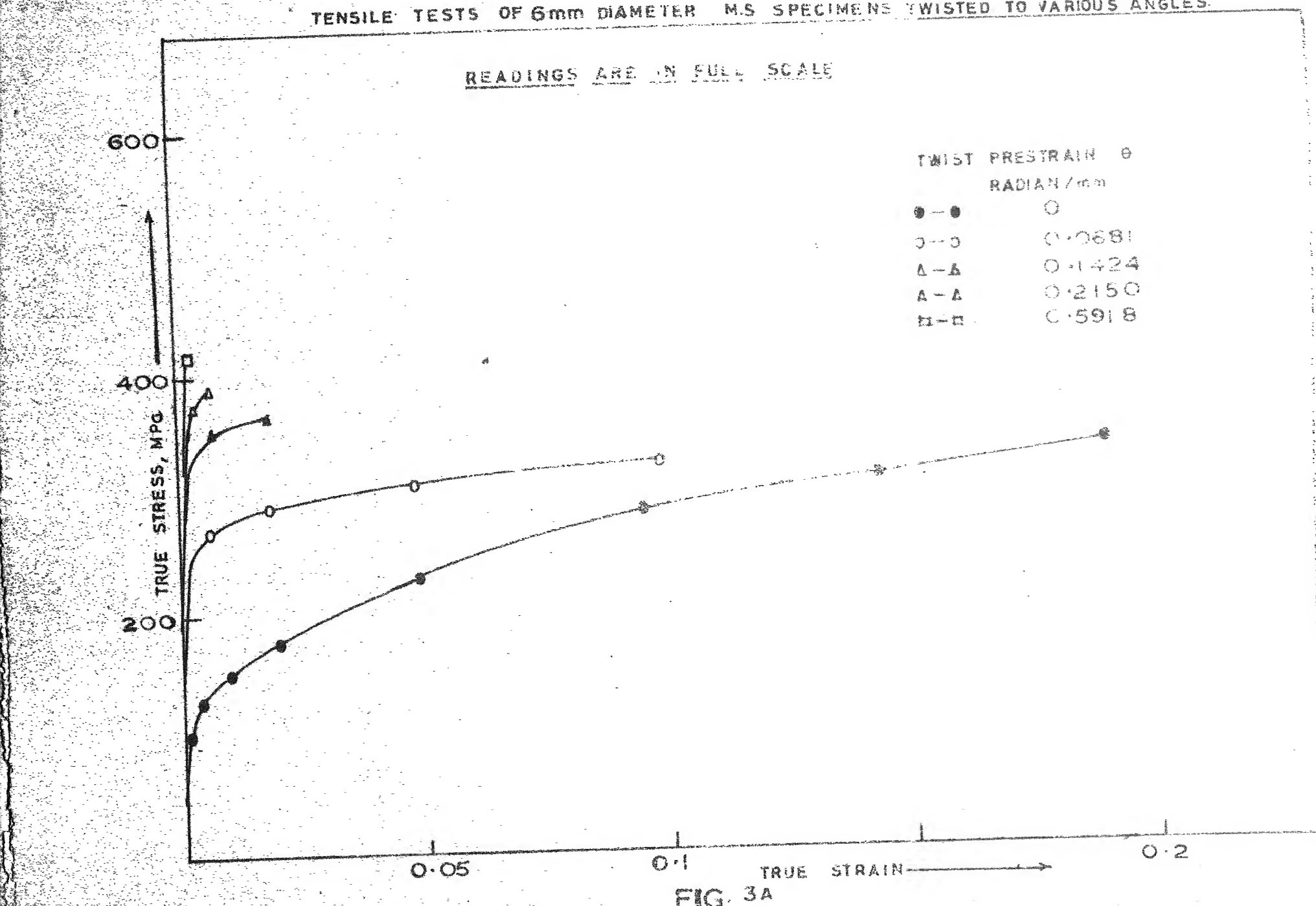

FIG. 3A

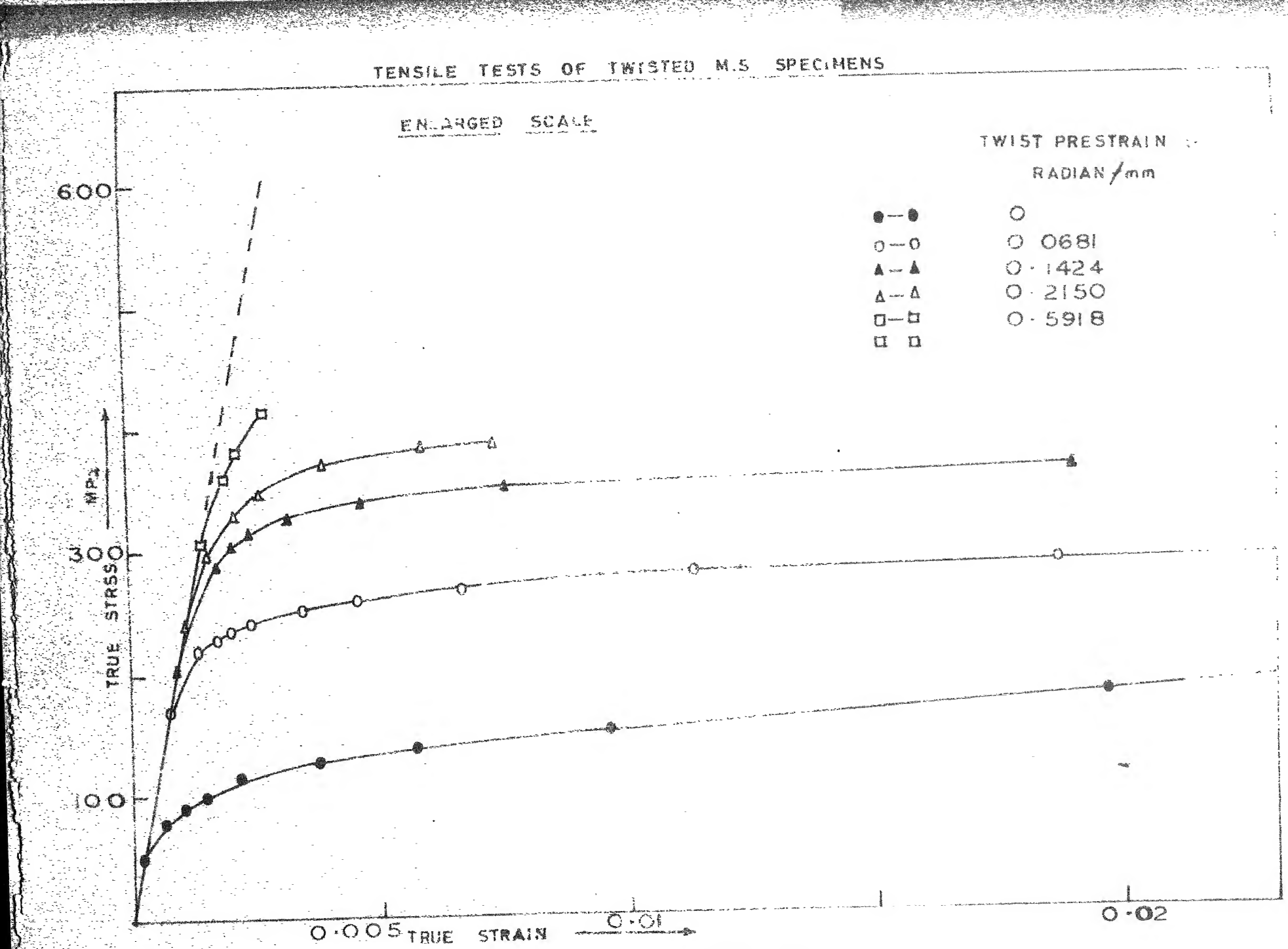
TENSILE TESTS OF TWISTED M.5 SPECIMENS
ENLARGED SCALE
TWIST PRESTRAIN :-
RADIAN/mm
0
0 0681
0 · 1424
0 · 2150
0 · 5918
600
300
100
TRUE STRSSO
MPa
0·005 TRUE STRAIN
0·01
0·02

FIG. 3B

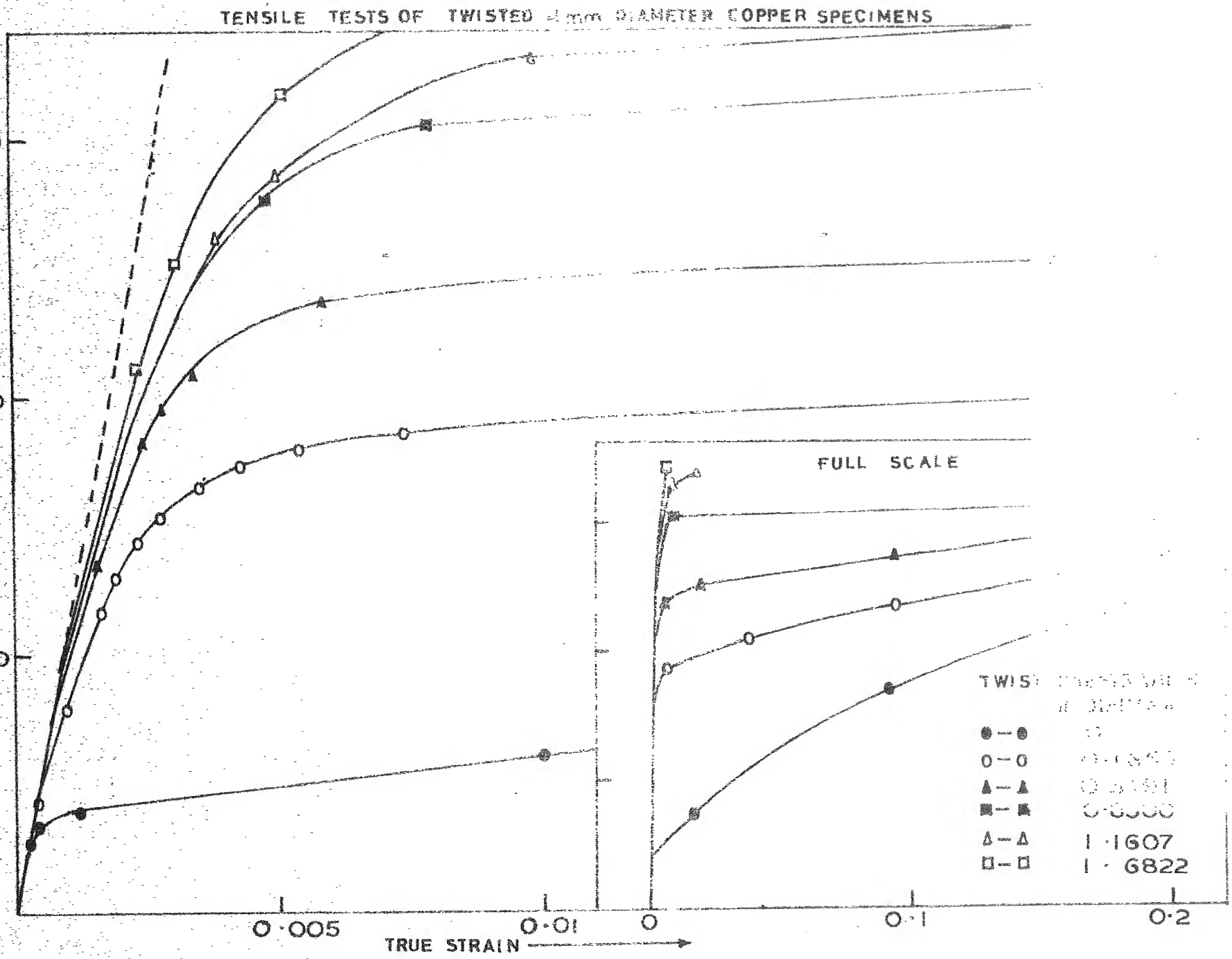
TENSILE TESTS OF TWISTED 4 mm DIAMETER COPPER SPECIMENS
300
200
100
TRUE STRSS MPa
FULL SCALE
TWIST
1·1607
1·6822
0·005
0·01
0
0·1
0·2
TRUE STRAIN

FIG. 4

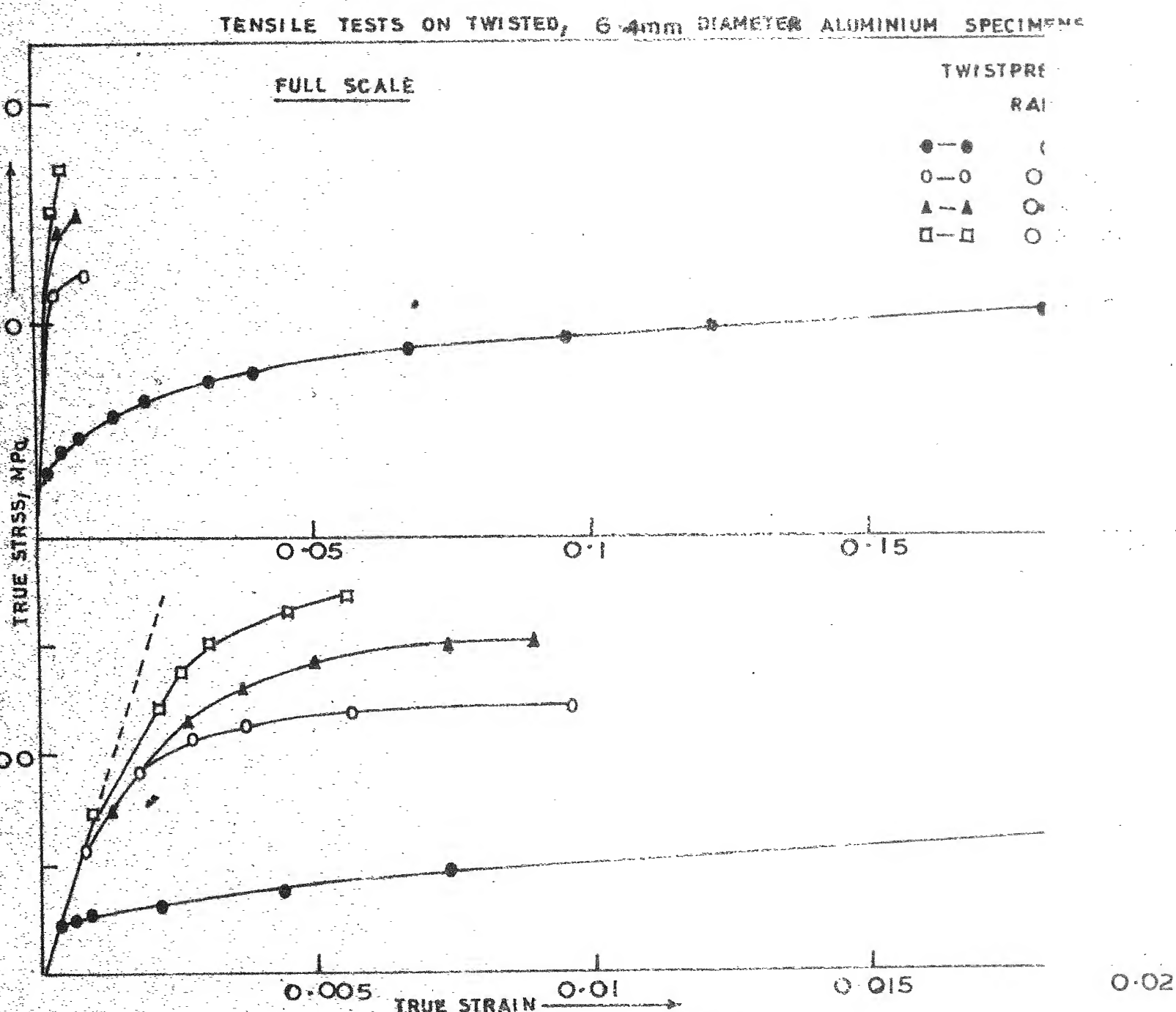
TENSILE TESTS ON TWISTED, 6·4mm DIAMETER ALUMINIUM SPECIMENS
FULL SCALE
TWISTPRE
RAI
200
100
TRUE STRESS, MPa
0·05
0·1
0·15
100
0·005
0·01
0·015
0·02
TRUE STRAIN

FIG. 5

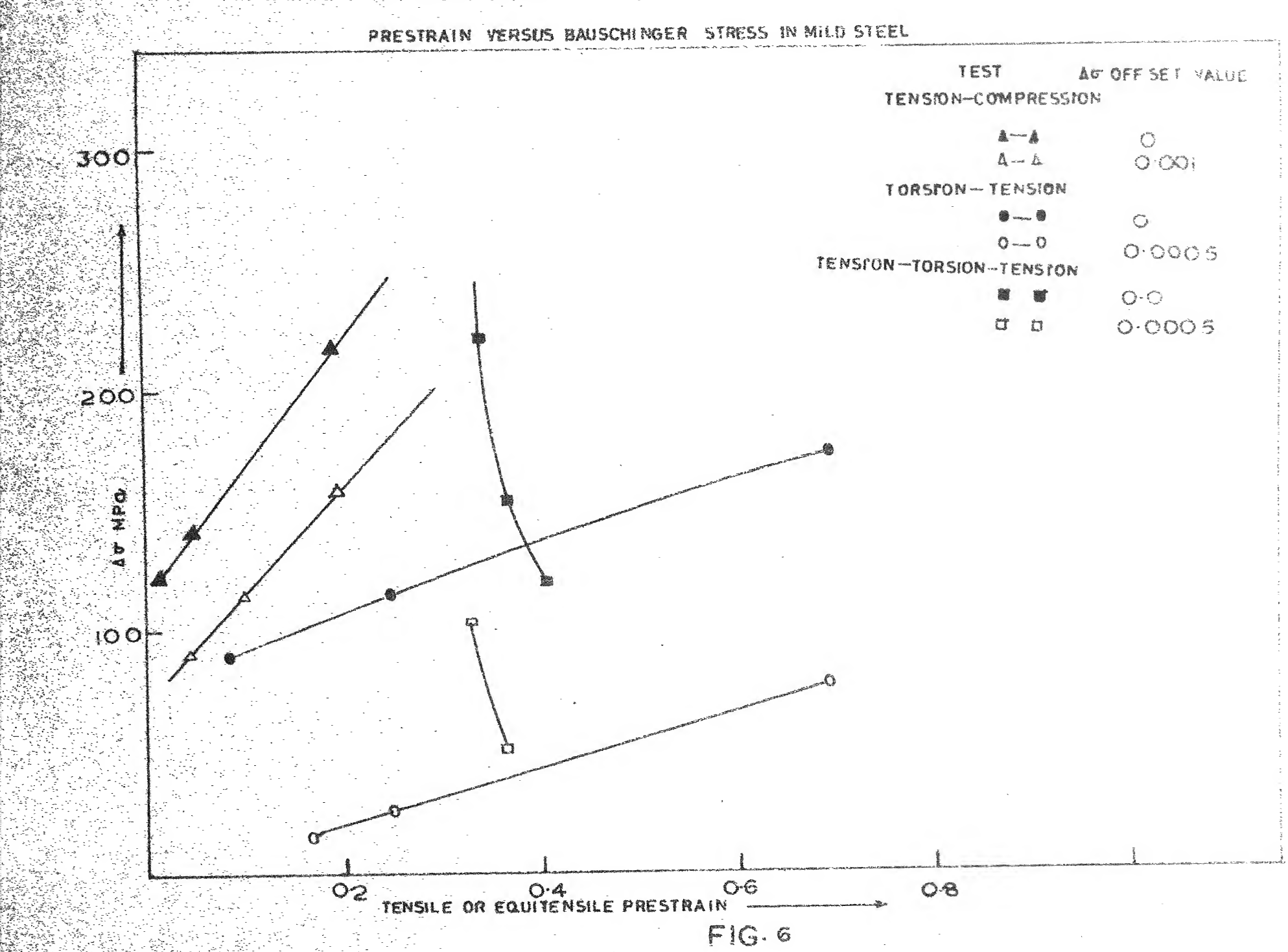
PRESTRAIN VERSUS BAUSCHINGER STRESS IN MILD STEEL
TEST
Δσ OFF SET VALUE
TENSION–COMPRESSION
0
0·001
TORSION – TENSION
0
0·0005
TENSION–TORSION–TENSION
0·0
0·0005
300
200
100
Δσ MPa
0·2
0·4
0·6
0·8
TENSILE OR EQUITENSILE PRESTRAIN

FIG. 6

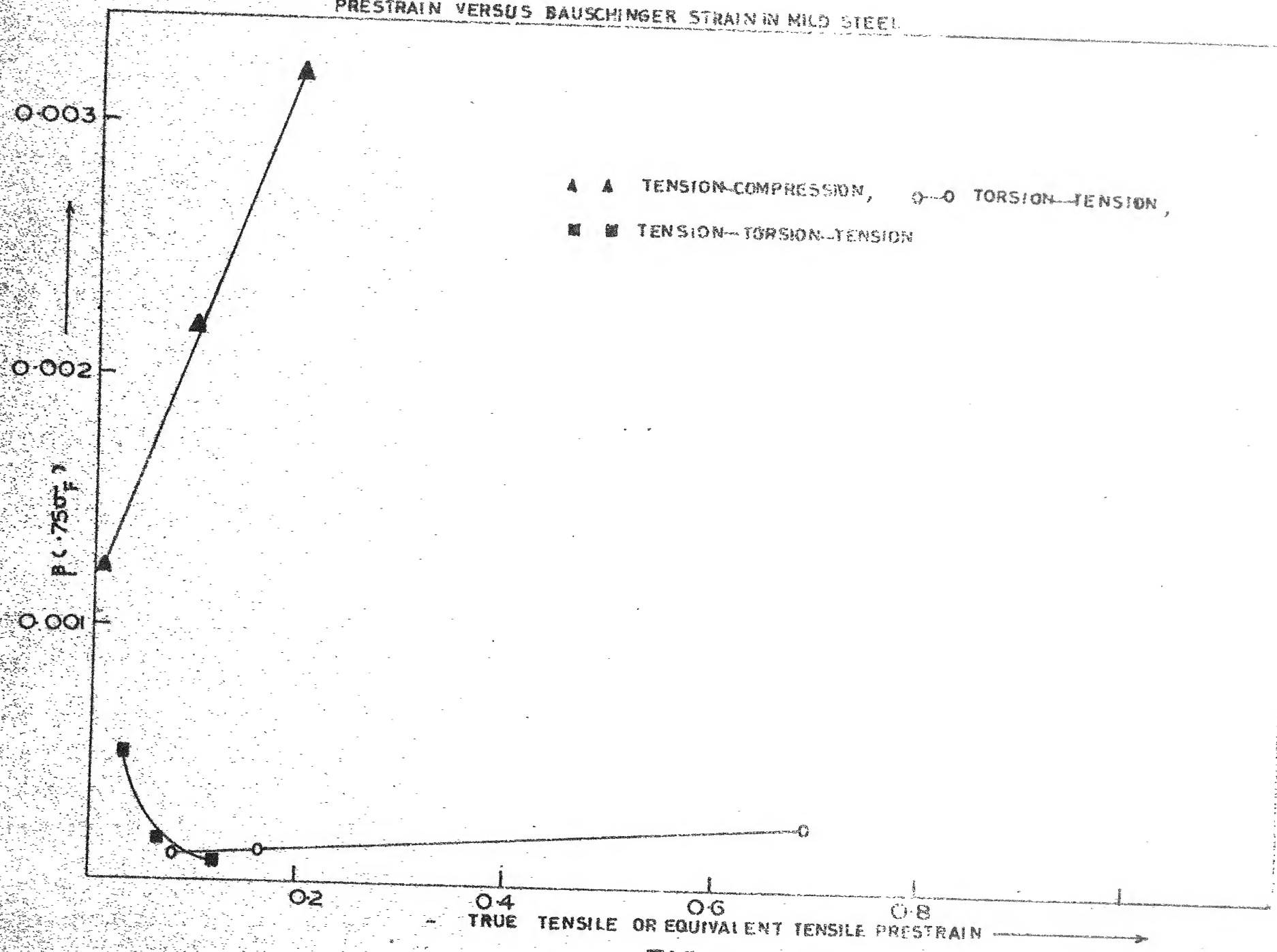
PRESTRAIN VERSUS BAUSCHINGER STRAIN IN MILD STEEL
0·003
0·002
0·001
P (·75σF)
▲ ▲ TENSION-COMPRESSION, o—o TORSION-TENSION,
■ ■ TENSION—TORSION-TENSION
0·2
0·4
0·6
0·8
TRUE TENSILE OR EQUIVALENT TENSILE PRESTRAIN

FIG. 7

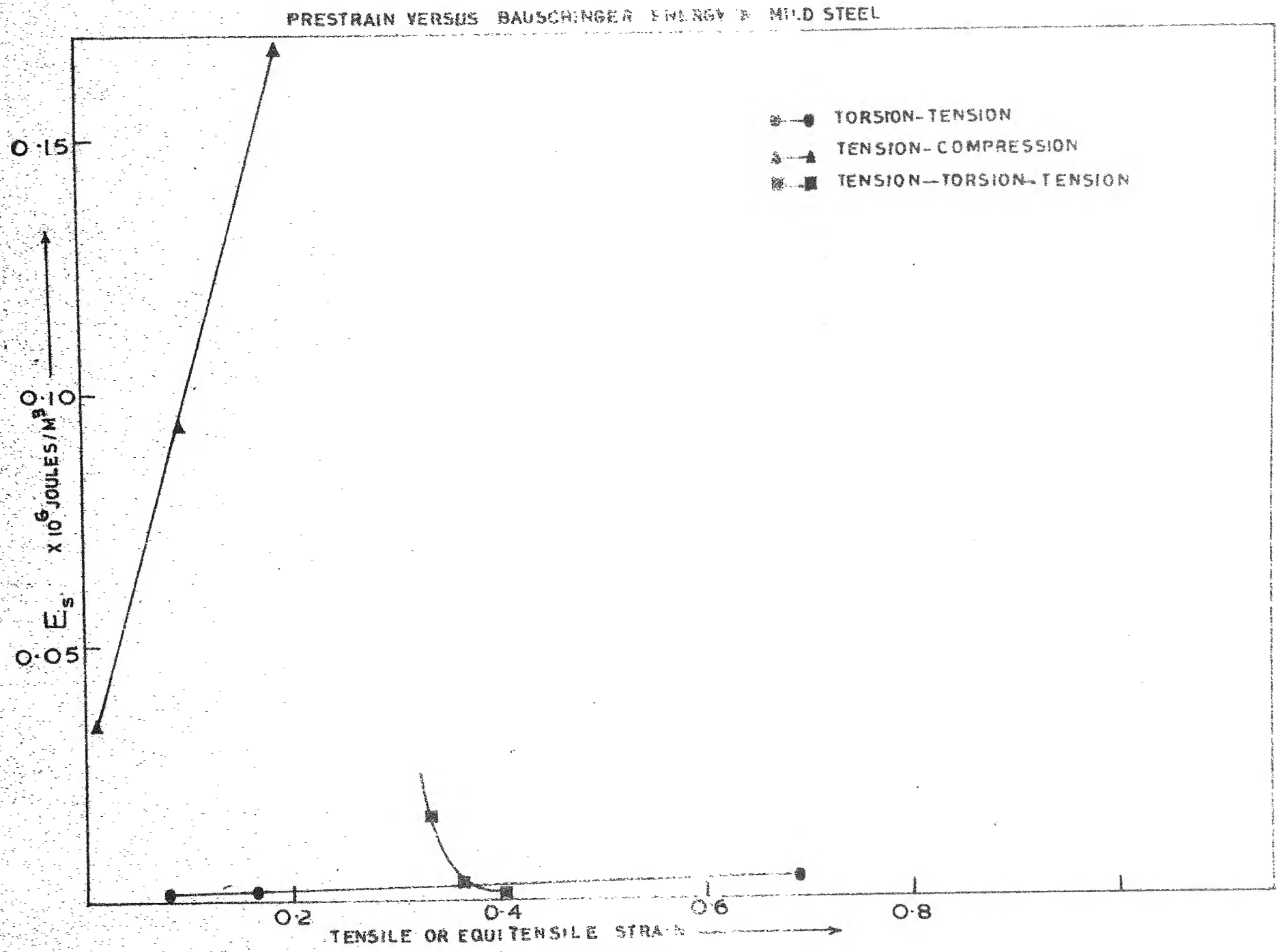
PRESTRAIN VERSUS BAUSCHINGER ENERGY IN MILD STEEL
TORSION-TENSION
TENSION-COMPRESSION
TENSION—TORSION-TENSION
0·15
0·10
0·05
E_s X 10^6 JOULES/M^3
0·2
0·4
0·6
0·8
TENSILE OR EQUITENSILE STRAIN

FIG. F

PRESTRAIN VERSUS BAUSCHINGER

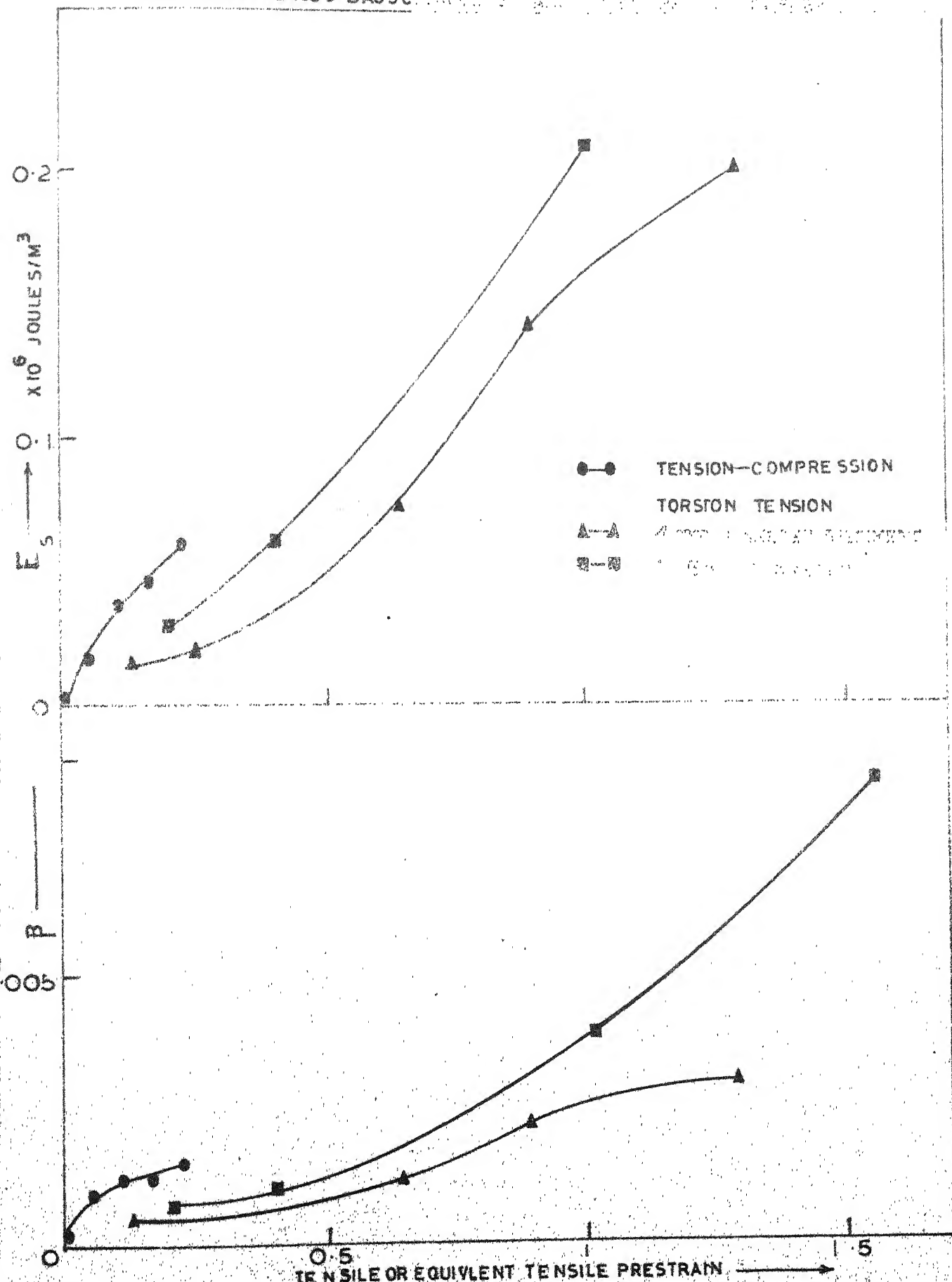

FIG. 10

BAUSCHINGER STRESS VERSUS RATE OF WORK-HARDENING IN MILD STEEL

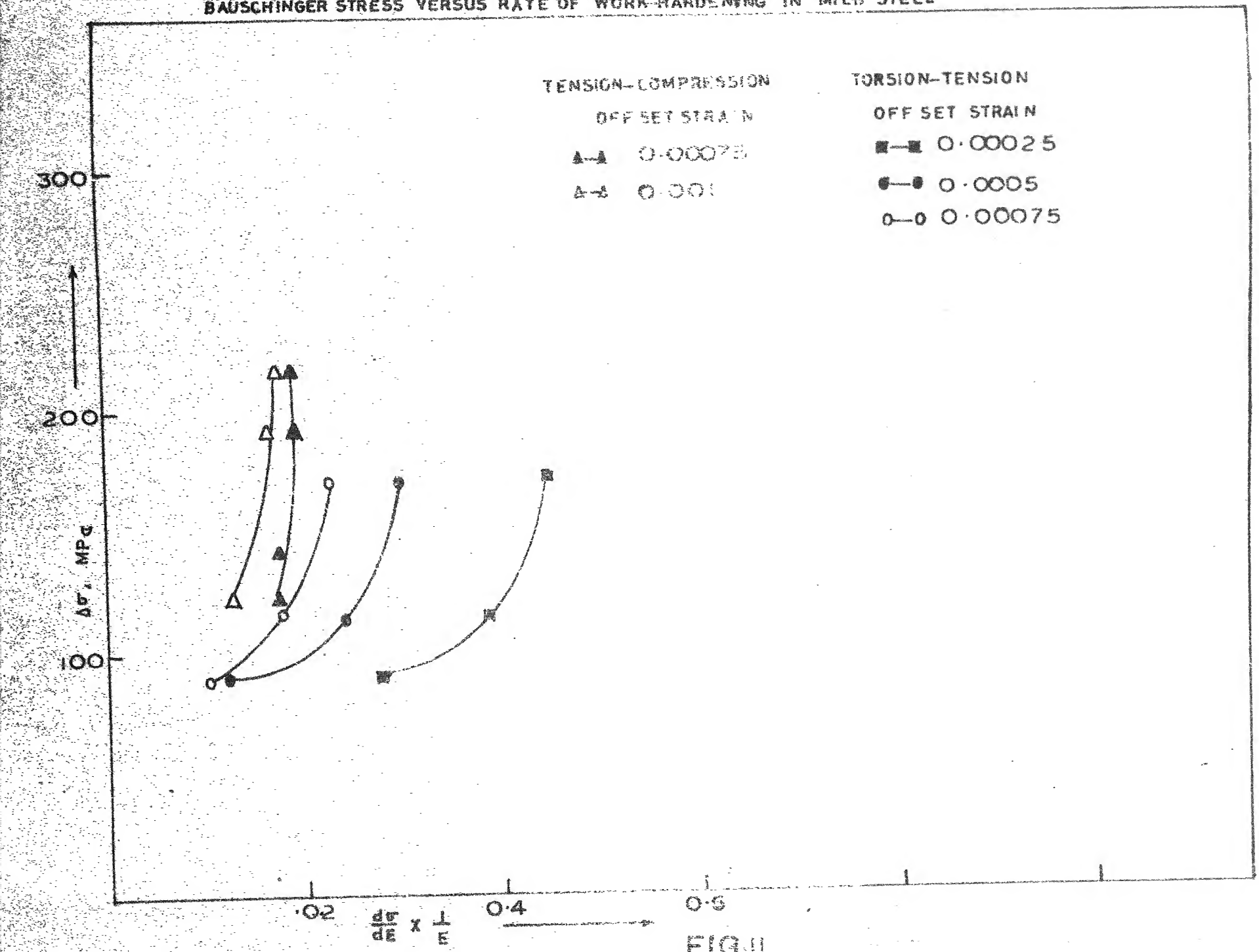

FIG 11

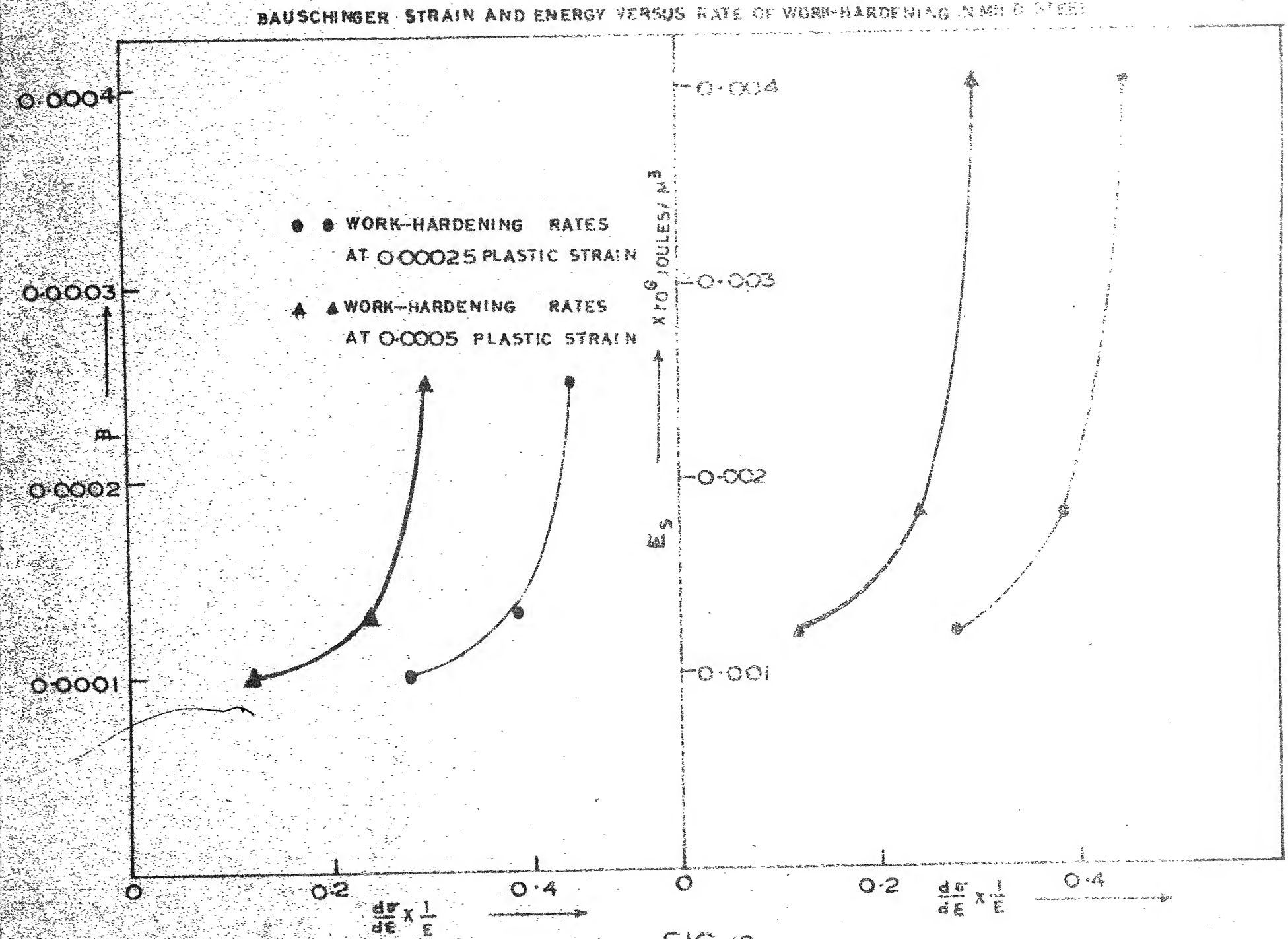
BAUSCHINGER STRAIN AND ENERGY VERSUS RATE OF WORK-HARDENING IN MILD STEEL
0·0004
0·0003
0·0002
0·0001
β
● ● WORK-HARDENING RATES AT 0·00025 PLASTIC STRAIN
▲ ▲ WORK-HARDENING RATES AT 0·0005 PLASTIC STRAIN
0·004
0·003
0·002
0·001
E_s X 10^9 JOULES/M^3
0
0·2
0·4
$\frac{d\sigma}{d\varepsilon} \times \frac{1}{E}$
0
0·2
$\frac{d\sigma}{d\varepsilon} \times \frac{1}{E}$
0·4

FIG. 12

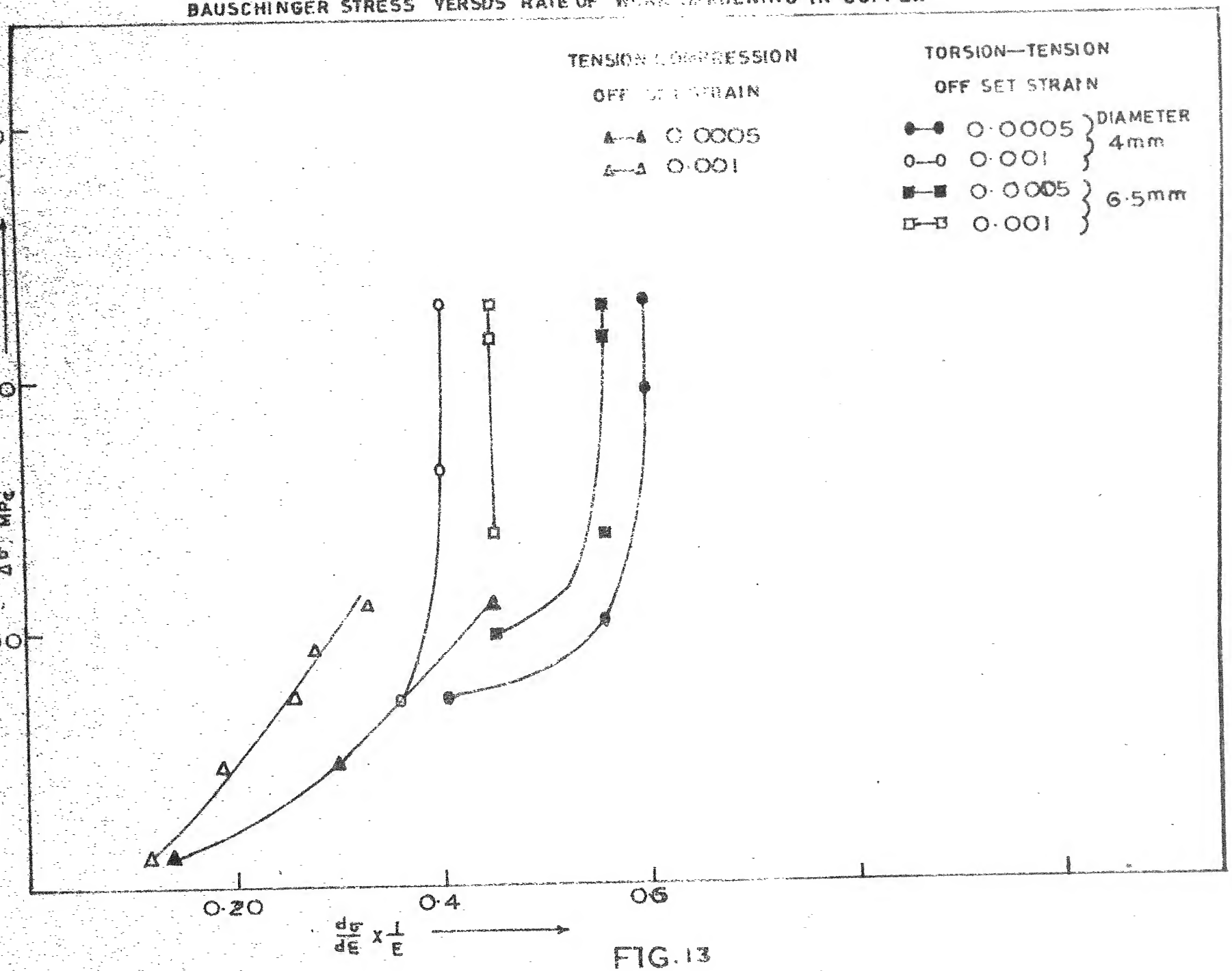
BAUSCHINGER STRESS VERSUS RATE OF WORK HARDENING IN COPPER
TENSION COMPRESSION
OFF SET STRAIN
0·0005
0·001
TORSION—TENSION
OFF SET STRAIN
0·0005
0·001
DIAMETER 4mm
0·0005
0·001
DIAMETER 6·5mm
300
200
100
Δσ, MPa
0·20
0·4
0·6
dσ/dε x 1/E

FIG. 13

BAUSCHINGER STRAIN AND ENERGY VERSUS RATE OF [illegible] IN COPPER

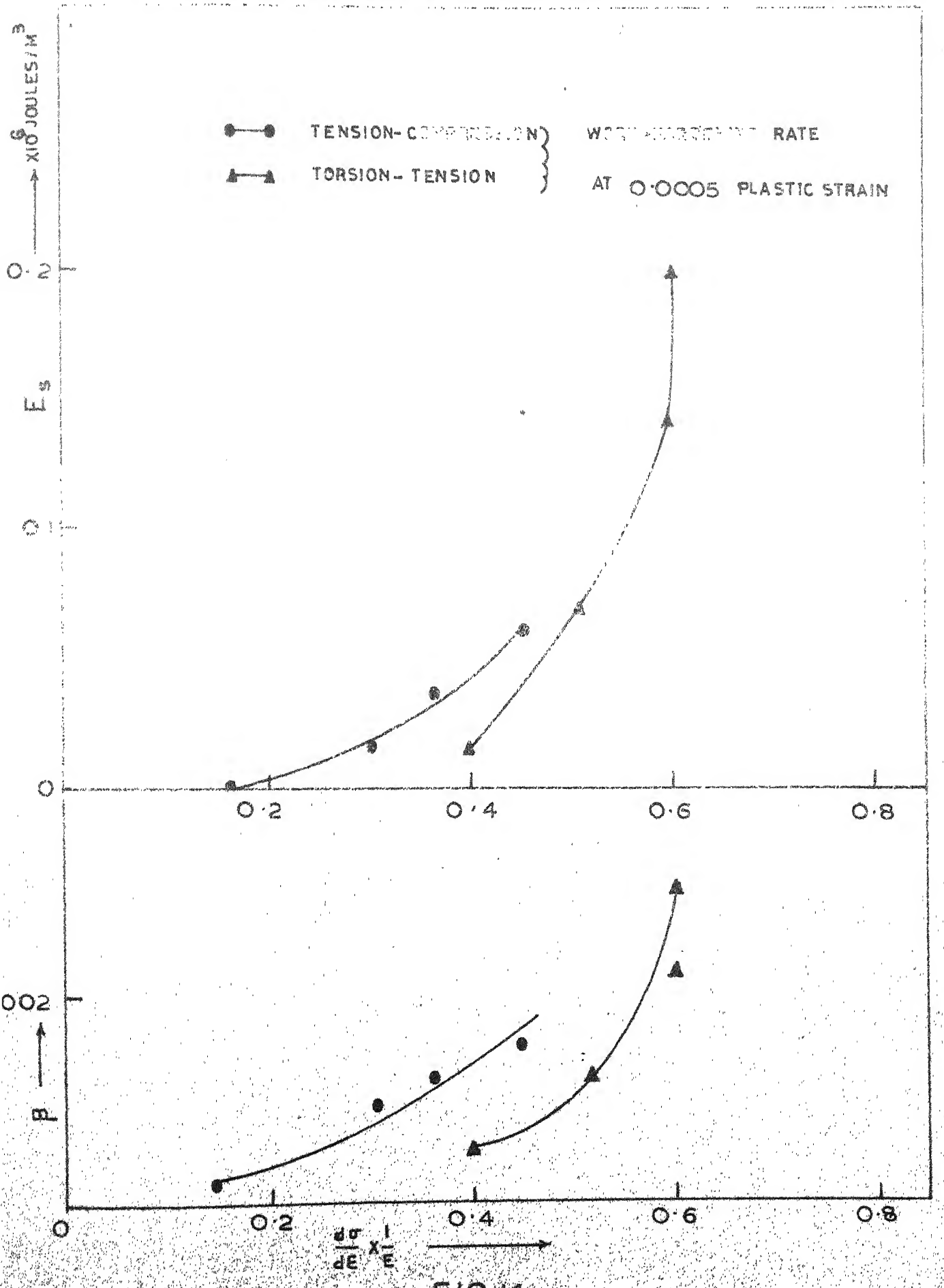

FIG. 14

TENSILE TESTS OF COMBINED PRESTRAINED MILD STEEL SPECIMENS

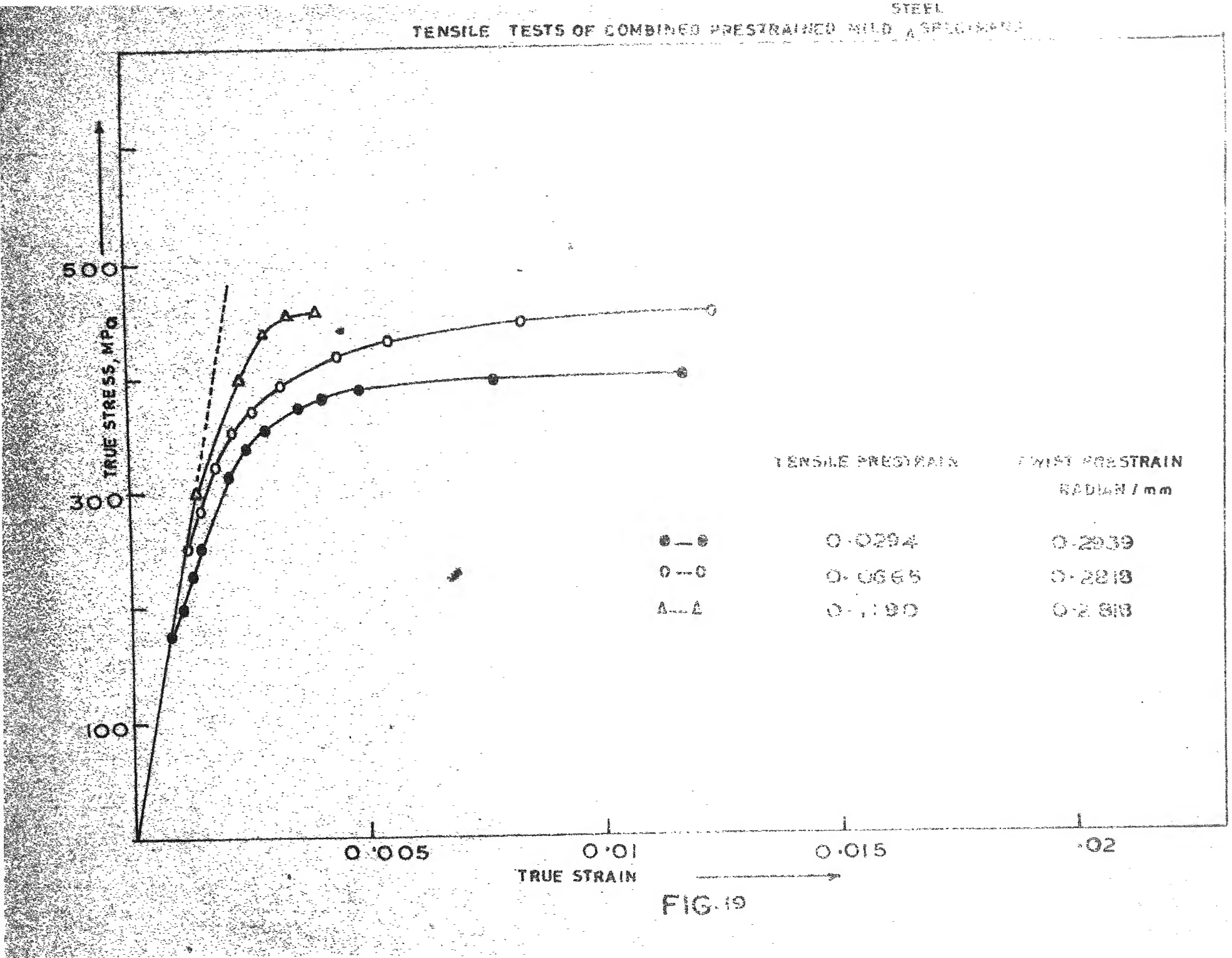

FIG. 19

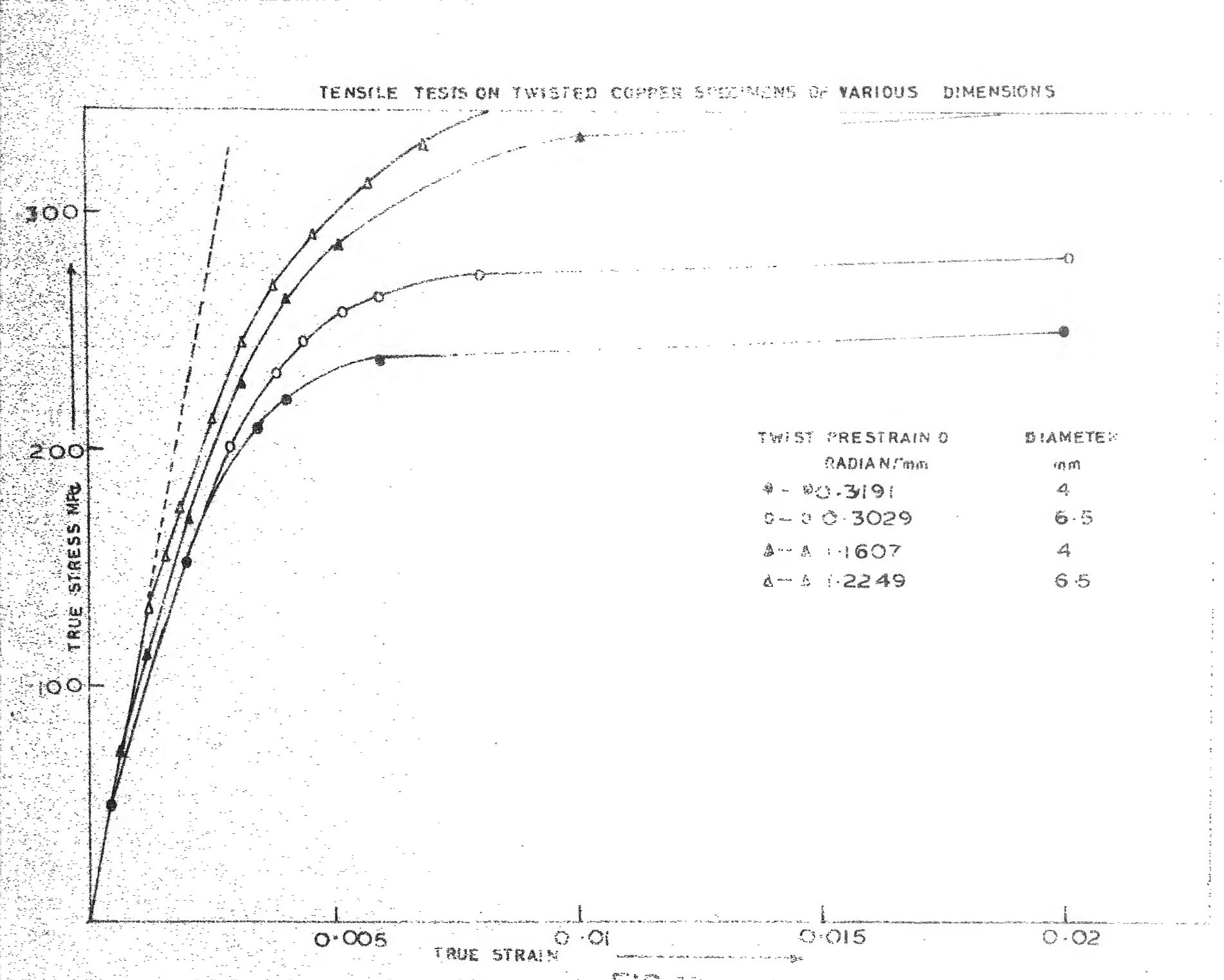
TENSILE TESTS ON TWISTED COPPER SPECIMENS OF VARIOUS DIMENSIONS
300
200
100
TRUE STRESS MPa
0·005
0·01
0·015
0·02
TRUE STRAIN
TWIST PRESTRAIN θ
RADIAN/mm
DIAMETER
mm
●—● 0·3191
4
○—○ 0·3029
6·5
▲—▲ 0·1607
4
△—△ 0·2249
6·5

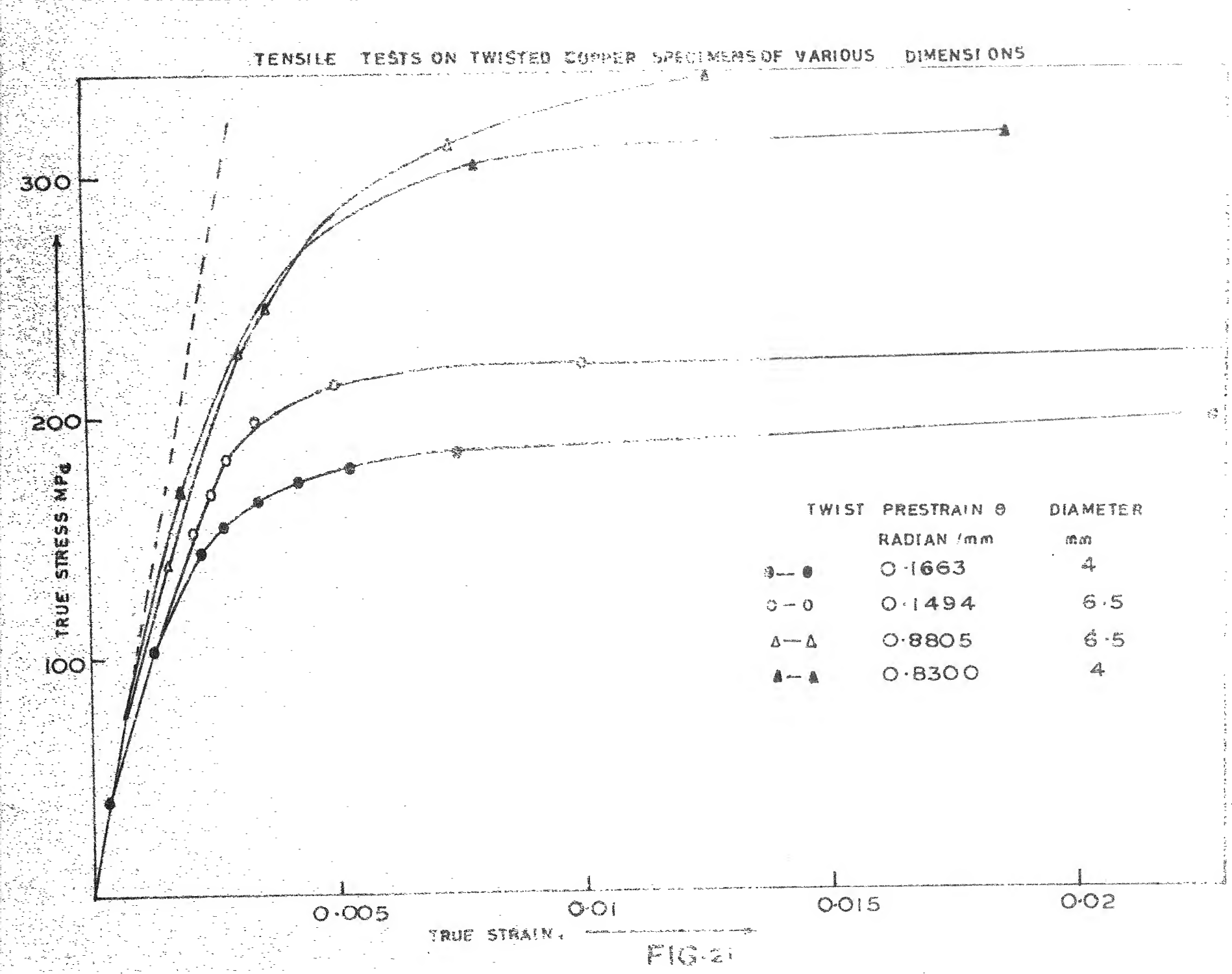
TENSILE TESTS ON TWISTED COPPER SPECIMENS OF VARIOUS DIMENSIONS
300
200
100
TRUE STRESS MPa
0·005
0·01
0·015
0·02
TRUE STRAIN
TWIST PRESTRAIN θ
RADIAN /mm
DIAMETER
mm
●—● 0·1663 4
○—○ 0·1494 6·5
△—△ 0·8805 6·5
▲—▲ 0·8300 4

FIG·2

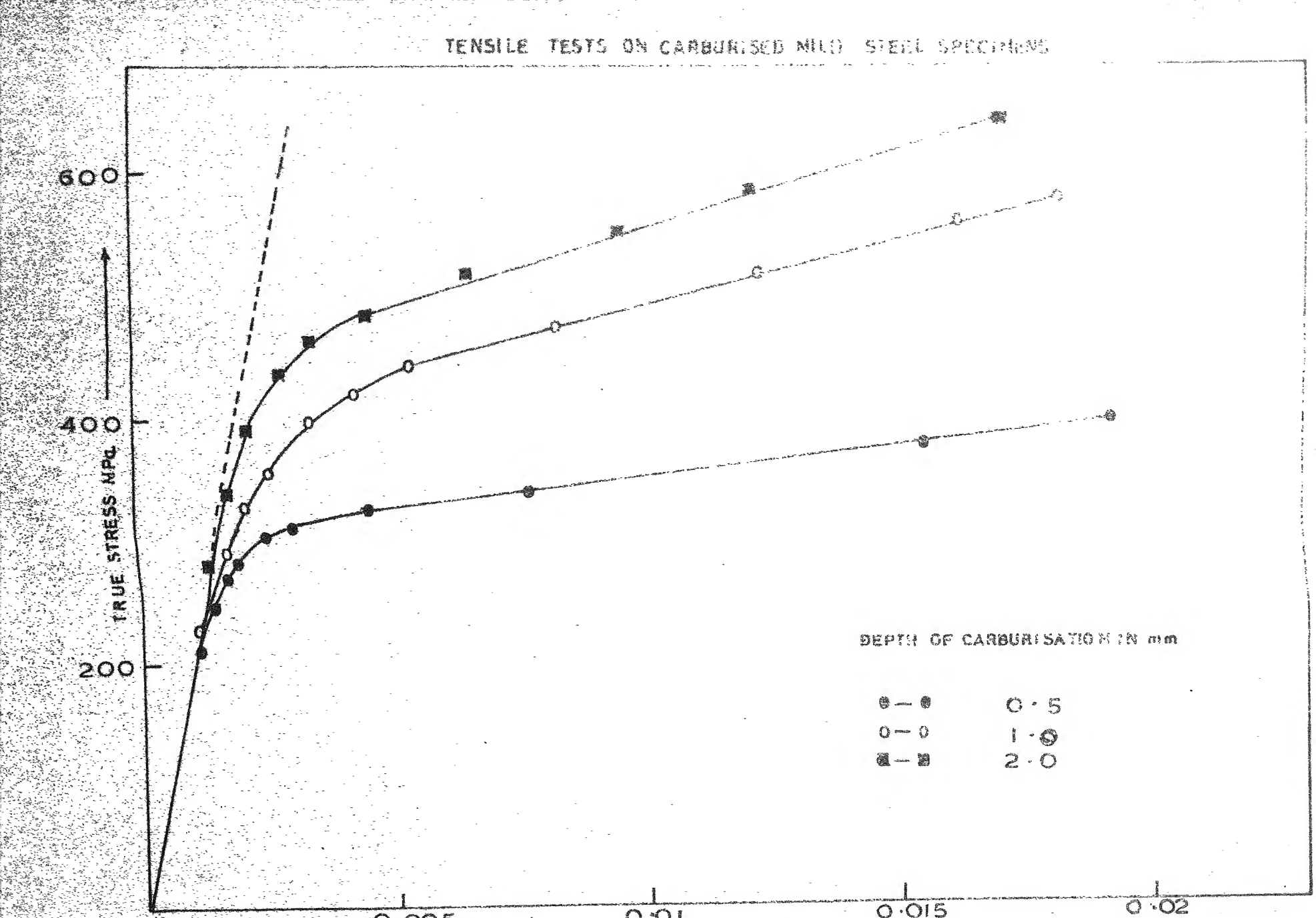
TENSILE TESTS ON CARBURISED MILD STEEL SPECIMENS
600
400
200
TRUE STRESS MPa
0·005
0·01
0·015
0·02
TRUE STRAIN
DEPTH OF CARBURISATION IN mm
0·5
1·0
2·0

FIG·22

WORK HARDENING RATE AT VARIOUS OFF SET STRAIN VALUES IN TENSION

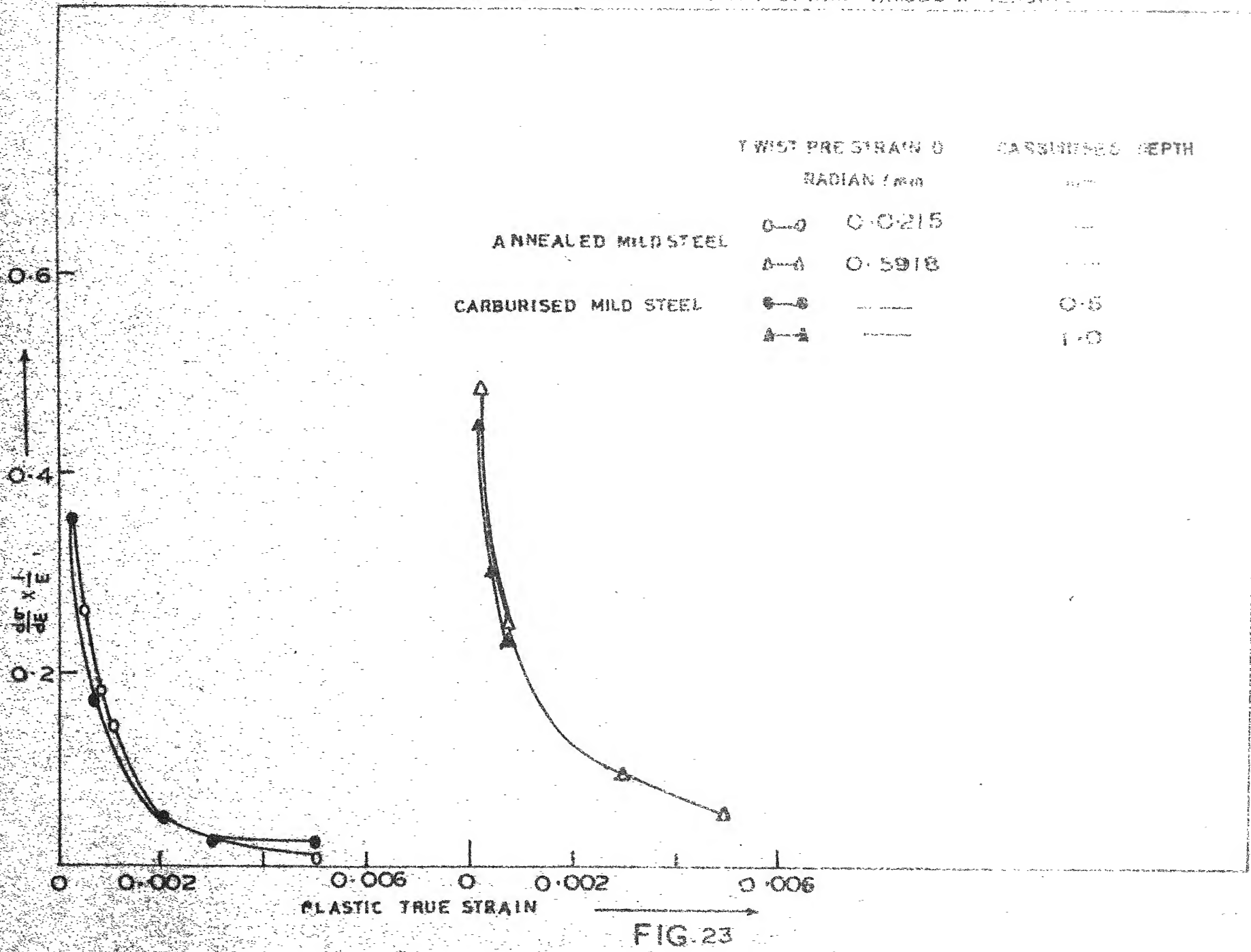

FIG. 23

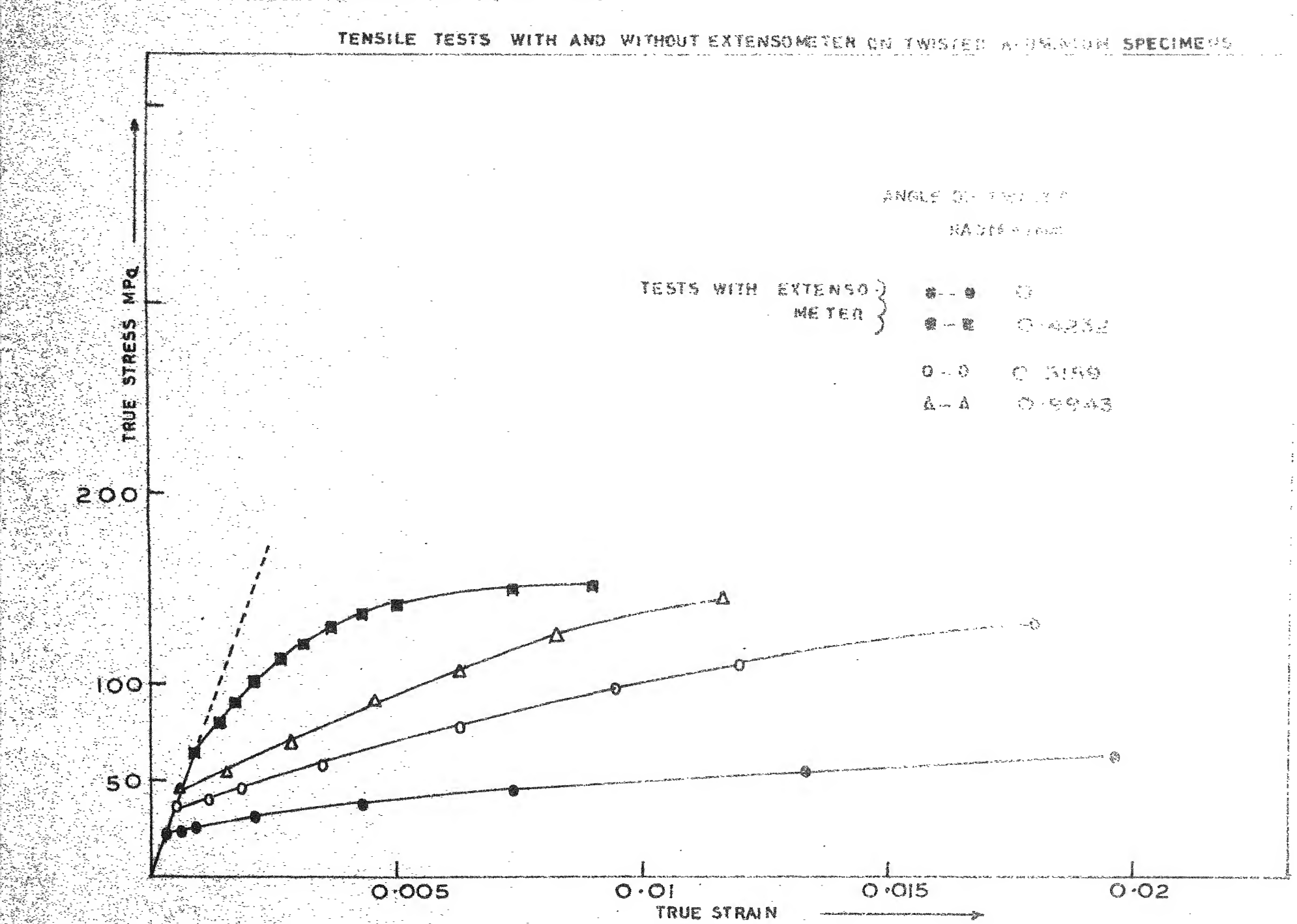
TENSILE TESTS WITH AND WITHOUT EXTENSOMETER ON TWISTED ADHESION SPECIMENS
TRUE STRESS MPa
200
100
50
0·005
0·01
0·015
0·02
TRUE STRAIN
TESTS WITH EXTENSO METER
0 - 0

FIG·24

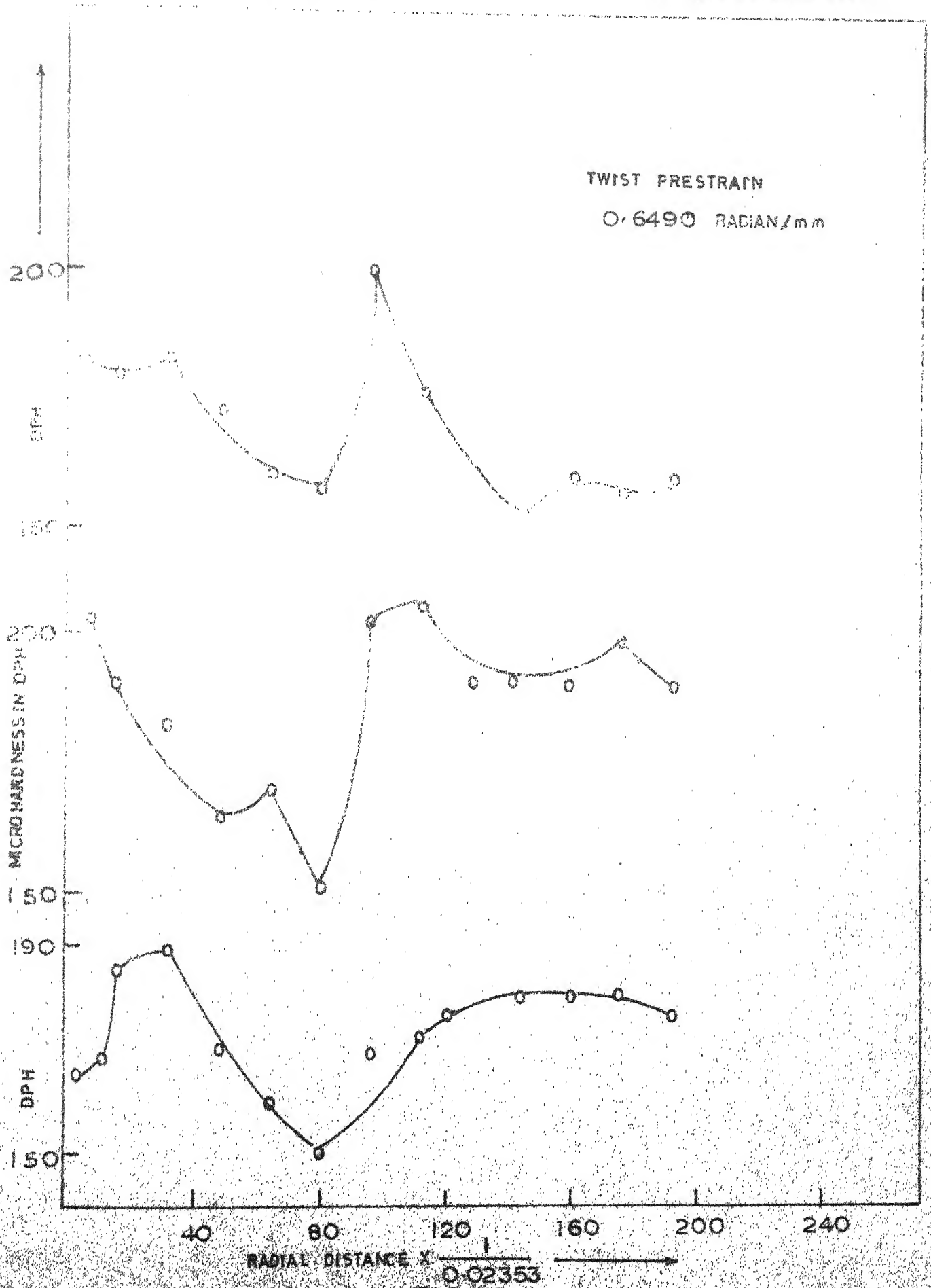
NUMBER VERSUS RADIAL
R TWISTED MILD STEEL
TWIST PRESTRAIN
0·6490 RADIAN/mm
200
150
MICRO HARDNESS IN DPH
150
190
DPH
150
40
80
120
160
200
240
RADIAL DISTANCE X 1/0.02353

FIG. 25

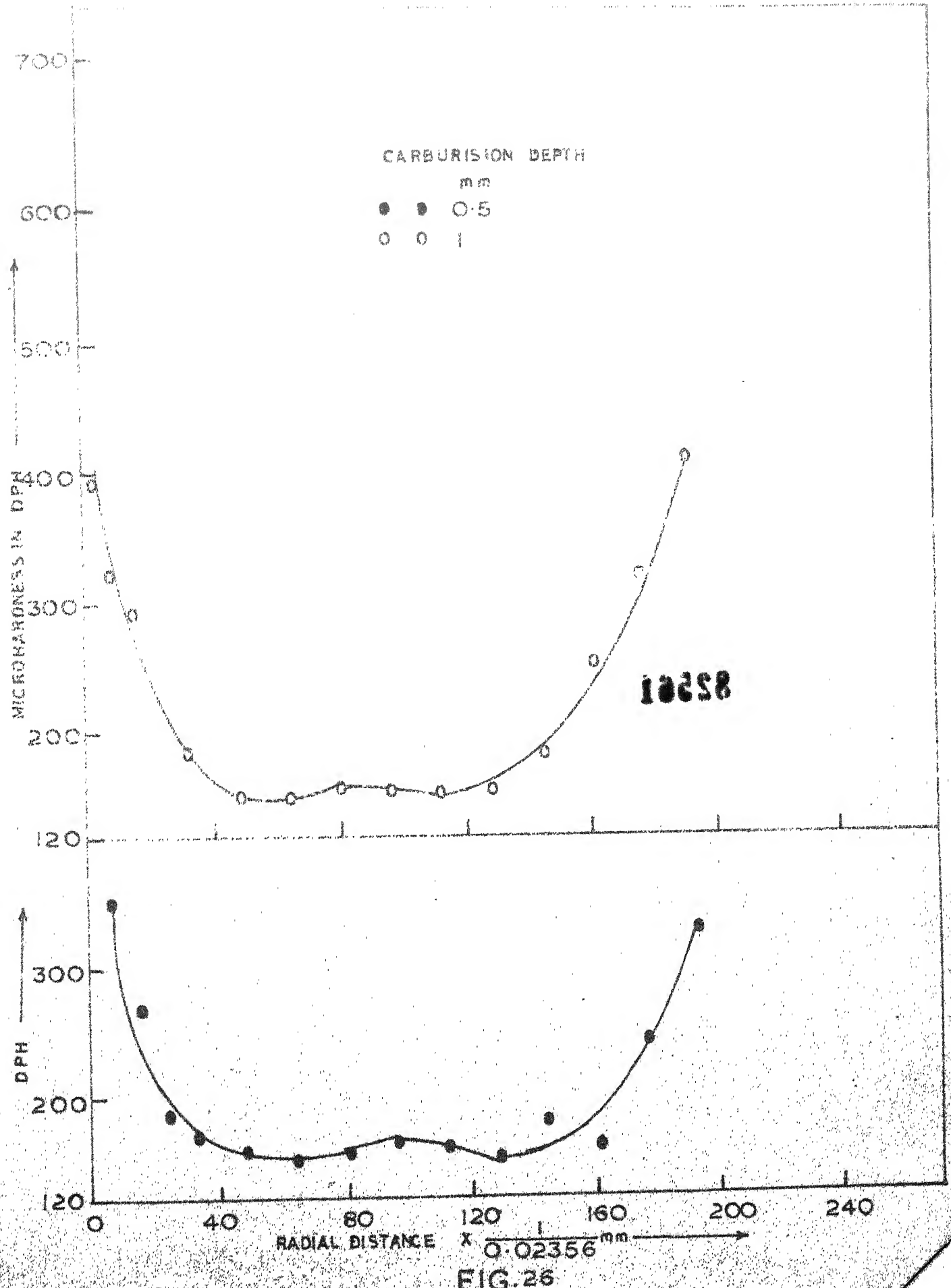
CARBURISION DEPTH
mm
0·5
1
MICRONARDNESS IN DPH
700
600
500
400
300
200
120
DPH
300
200
120
0
40
80
120
160
200
240
RADIAL DISTANCE x 1/0·02356 mm

FIG. 26